Indian Monsoon GCM Sensitivity Experiments Testing Tropospheric Biennial Oscillation Transition Conditions

GERALD A. MEEHL AND JULIE M. ARBLASTER

National Center for Atmospheric Research, Boulder, Colorado*

(Manuscript received 15 March 2001, in final form 31 October 2001)

ABSTRACT

Observational studies have shown that the tropospheric biennial oscillation (TBO) involves transitions that occur from northern spring [March–April–May (MAM)] to the Indian monsoon season [June–July–August–September (JJAS)] such that a relatively strong monsoon the previous year is often followed by a relatively weak one, and vice versa. Several conditions involving anomalous land and ocean surface temperature anomalies in the Indo-Pacific region in MAM have been identified to be associated with TBO monsoon transitions. Though it is possible to quantify the *relative* contribution of each transition condition year by year in observations, they are interrelated and the question remains whether each condition *by itself* could cause a monsoon transition. Here, a series of GCM sensitivity experiments is performed to isolate the effects of each of the transition conditions to document their respective influences on the anomalous patterns of monsoon rainfall associated with TBO transitions. Three conditions postulated to contribute to these TBO transitions associated with Indian monsoon rainfall are 1) atmospheric circulation–related anomalous south Asian land temperatures and resulting meridional temperature gradients, 2) anomalous SSTs in the Indian Ocean, and 3) anomalous tropical Pacific SSTs. Sensitivity experiments with an atmospheric GCM (the NCAR CCM3) are performed to address these conditions by specifying 1) warmer land temperatures over Asia to produce a stronger meridional temperature gradient, 2) warm Indian Ocean SST anomalies, and 3) cold Pacific Ocean SST anomalies. The model results demonstrate that each of the transition conditions is associated with distinct physical processes and can contribute to a relative TBO transition in monsoon strength by themselves. The anomalous tropical Indian and Pacific Ocean SST anomalies produce a larger monsoon response in the model compared to the anomalous meridional temperature gradient over Asia indicating they are the dominant conditions associated with TBO transitions. The location of the SST anomalies over the tropical Indian Ocean is important, with warm SST anomalies throughout the tropical Indian Ocean producing enhanced rainfall over the ocean and south Asian land areas, and warm SST anomalies near the equatorial Indian Ocean producing increased rainfall locally with decreased rainfall over south Asian land areas. Case studies from observations illustrate that the various transition conditions are evident in the raw data in individual years. Several more GCM experiments are performed to show how some conditions can act cumulatively to produce monsoon transitions.

1. Introduction

For the Asian–Australian monsoon, the tropospheric biennial oscillation (TBO) is defined as the tendency for a relatively strong monsoon to be followed by a relatively weak one, and vice versa, with the transitions occurring in the season prior to the monsoon involving coupled land–atmosphere–ocean processes over a large area of the Indo-Pacific region (Meehl 1987, 1993, 1994, 1997; Meehl and Arblaster 2001, 2002). Thus the TBO is not so much an oscillation, but a tendency for the system to flip-flop back and forth from year to year. The more of these interannual flip-flops or transitions, the more biennial the system. Various parts of this system have been studied previously for mechanisms related to the TBO (e.g., Chang and Li 2000; Clarke et al. 1998; Clarke and Shu 2000; Li and Yanai 1996; Rao and Goswami 1988; Tomita and Yasunari 1996; Yasunari and Seki 1992; Webster et al. 1998, 1999; Kim and Lau 2001).

Meehl and Arblaster (2001, 2002), following up earlier studies by Meehl (1987, 1997), showed that certain conditions in the seasons prior to the monsoon, set up by coupled interactions in the preceding year, will cause the monsoon to be relatively stronger (or weaker) than the previous or following years, thus introducing a biennial component in spectra of area-averaged monsoon rainfall. These conditions include anomalous SSTs in the Indian and Pacific Oceans for both the south Asian and Australian monsoons, in addition to anomalous me-

* The National Center for Atmospheric Research is sponsored by the National Science Foundation.

Corresponding author address: Dr. Gerald A. Meehl, National Center for Atmospheric Research, P.O. Box 3000, Boulder, CO 80307-3000.
E-mail: meehl@ncar.ucar.edu

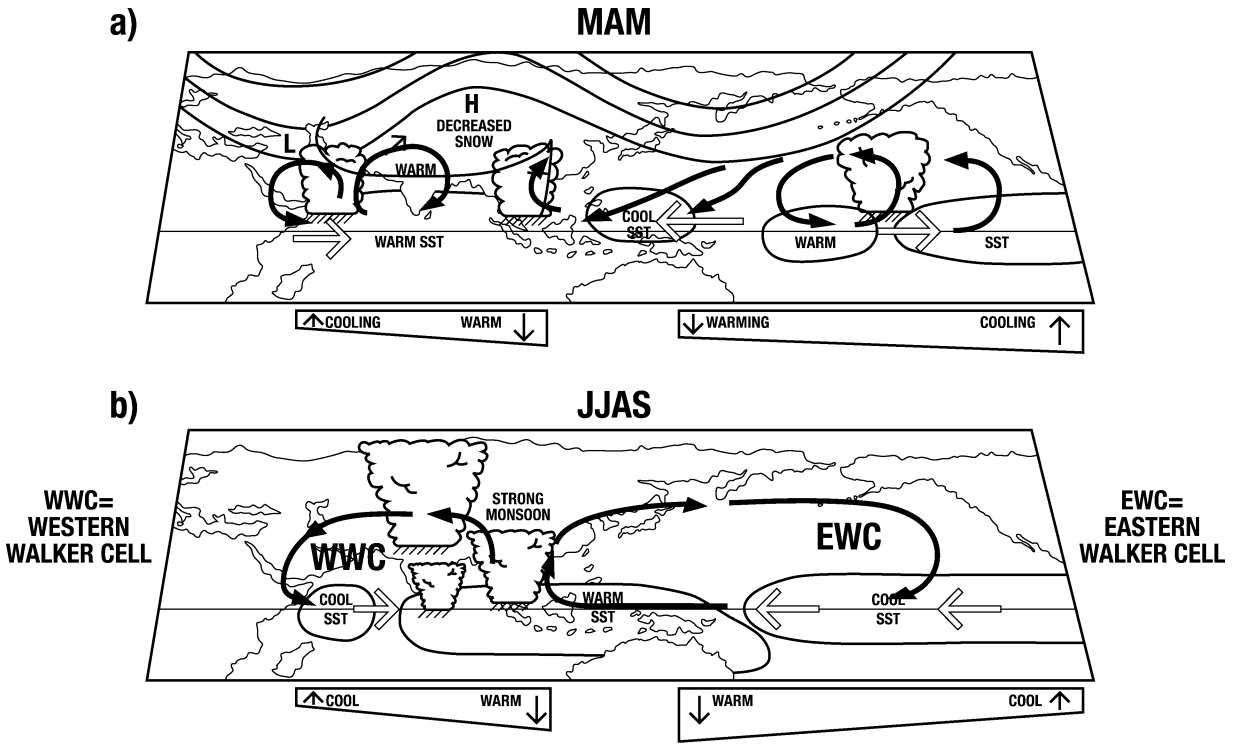

FIG. 1. Schematic diagram indicating anomalous convective activity. SST anomalies, midlatitude circulation anomalies, surface wind anomalies, and equatorial Indian and Pacific Ocean thermocline orientation for hypothesized TBO transition for (a) the MAM season before a strong Indian monsoon, and (b) strong Indian monsoon season, JJAS. Large arrows indicate surface wind anomalies, wedge-shaped outlines below each panel represent anomalous thermocline orientation, with the small arrows in those areas indicative of anomalous movement of the thermocline, and wavy arrows indicating Kelvin waves with arrow at the end representing upwelling Kelvin waves (arrow pointing up), or downwelling Kelvin waves (arrow pointing down; after Meehl and Arblaster 2002). Thick black arrows indicate the eastern and western Walker cells labeled in (b) as EWC and WWC, respectively.

ridional temperature gradients over Asia prior to the Indian monsoon. They provided evidence from singular value decomposition (SVD) analyses of observations for the period 1979–99. They also noted that use of first SVD modes does not guarantee orthogonality and, in fact, all the transition conditions, particularly Indian and Pacific SSTs, are related. Consequently, they used single and cumulative pattern correlation techniques to quantify the separate contributions of the transition conditions year by year. They showed that in some years the transition conditions were related, and in others they were not. The point was they quantified, for each year, the magnitude of the contribution from each of the three transition conditions. However, it was unclear from those analyses whether the first SVD components were physically distinct or simply artifacts of the analyses. Therefore, the purpose of this paper is to perform GCM experiments specifying conditions identified by Meehl and Arblaster (2001, 2002) to test the hypothesis that those conditions could each, by themselves, influence the [June–July–August–September (JJAS)] Indian monsoon rainfall in ways physically consistent with the SVD analyses. We first review the SVD results from Meehl and Arblaster (2001, 2002), and then perform ensemble GCM simulations with each condition separately.

Details for the TBO transition from March–April–May (MAM) to a relatively strong monsoon in JJAS compared to the previous year are shown in the hypothesized evolution for the TBO in Fig. 1 (after Meehl and Arblaster 2002). In the MAM season prior to a strong Indian monsoon (Fig. 1a), the convective heating anomalies associated with the precipitation and SST anomalies can contribute to an anomalous ridge over Asia and warm land temperatures there. Upwelling Kelvin waves from the easterly anomaly winds in the western Pacific that started in December–January–February (DJF) and continue during MAM act to raise the thermocline in the central and eastern Pacific thus providing the conditions for a transition in sign of SST anomalies from relatively warm in MAM to relatively cold in JJAS. In the Indian Ocean, westerly anomaly winds along the equator associated with stronger convection in the western Indian Ocean act to raise the thermocline in the west and lower it in the east, and contribute to warm SST anomalies over most of the central and eastern tropical Indian Ocean.

During JJAS in this hypothesized evolution (Fig. 1b), convection and precipitation over the Indian monsoon region are strong (note in this definition of the monsoon, land and ocean precipitation in the Indian region are

included, the sum of which are presumed to be dynamically important for the TBO). The eastern and western Walker cells are anomalously strong, winds over the equatorial Indian Ocean remain westerly, and the shallow thermocline in the west is evidenced by anomalously cool SSTs appearing in the western equatorial Indian Ocean. This is the beginning of a dipole of SSTs across the equatorial Indian Ocean, cool in the west and warm in the east. In the east there is a deep thermocline associated with the warm SST anomalies. Heavy rainfall over parts of the Asian land areas contributes to cooler land temperatures. There are strong trades, a shallow thermocline and cool SSTs in the central and eastern equatorial Pacific in JJAS, thus completing the SST transition there that began the previous DJF. In association with those negative SST anomalies in the east, there is a deep thermocline and warm SSTs in the western equatorial Pacific.

A number of previous model studies have attempted to address the role of anomalous surface conditions in contributing to monsoon precipitation. Early experiments by Shukla (1975) and Washington et al. (1977) showed that SST anomalies in the Indian Ocean could affect monsoon precipitation mainly through changes in evaporation and low-level moisture source. Palmer et al. (1992) successfully simulated many of the rainfall features of the Indian monsoons of 1987 and 1988 in a GCM with observed specified SSTs for those two years. They also isolated SST forcing from the Indian and Pacific Oceans, respectively, and showed that, for those two monsoon seasons, the Pacific SSTs were dominant over the Indian SSTs in contributing to the Indian monsoon rainfall anomalies. Yamazaki (1988) and Chandrasekar and Kitoh (1998) specified positive SST anomalies near the equatorial Indian Ocean and showed a local increase of precipitation but a reduction in monsoon rainfall over south Asian land areas. These studies illustrate the importance of location of Indian Ocean SST anomalies to subsequent monsoon rainfall as noted in the observations (e.g., Clark et al. 2000). Ju and Slingo (1995), Yang et al. (1996), and Soman and Slingo (1997) analyzed Atmospheric Model Intercomparison Project (AMIP) runs with specified observed SSTs to study relationships between regional SST anomalies in the Indian and western Pacific Oceans and large-scale forcing from eastern equatorial Pacific SST anomalies. Lau and Bua (1998) and Yang and Lau (1998) performed model experiments where land surface or SST conditions were specified. They showed that the effects of anomalous SSTs were dominant, with land surface conditions playing a secondary role but with important effects regionally. All of these experiments point to the various roles of SST and land surface temperature anomalies resulting in anomalous evaporation and convection that, in association with anomalous circulation patterns, ultimately affect monsoon rainfall. In this paper, three conditions (anomalously cool tropical Pacific SSTs, anomalously warm Indian Ocean SSTs, or anomalously strong meridional temperature gradients over Asia) will be specified in GCM sensitivity experiments and examined for their possible individual contributions to a relatively strong Indian monsoon.

In section 2 we describe the model and the observational data we use to compare with the model data. In section 3 we summarize the results from Meehl and Arblaster (2001, 2002) to provide the context for the model experiments, which are then discussed in section 4. In section 5 we pick individual years from the observations as case studies to illustrate the various conditions and associated monsoon characteristics shown in the model experiments. Section 6 follows with conclusions.

2. Data and model description

To compare to the model output, we use 21 yr of observed data for the period January 1979–October 1999 from the gridded Climate Prediction Center (CPC) Merged Analysis of Precipitation (CMAP) data (Xie and Arkin 1996), and atmospheric and surface temperature data from the National Centers for Environmental Prediction–National Center for Atmospheric Research (NCEP–NCAR) reanalysis data (Kalnay et al. 1996; Trenberth et al. 2001) for those same years. Therefore, there are 21 Indian monsoon years (1979–99) available for analysis. All data are on a T42 grid.

The atmospheric GCM used for the sensitivity experiments is the NCAR Community Climate Model 3 (CCM3) with T42 resolution (roughly 2.5° by 2.5°) and 18 levels in hybrid coordinates (Kiehl et al. 1998). The land surface model (LSM) included in CCM3 takes into account vegetation types and many surface processes (Bonan 1998). The atmospheric model's features of Asian–Pacific climate simulation with both specified SSTs (the version used here) and coupled to a dynamical ocean model are documented by Meehl and Arblaster (1998). Lal et al. (2000) also have looked at monsoon conditions in the version of this model coupled to a dynamical ocean.

3. TBO transition conditions from MAM to JJAS

As described above, Meehl and Arblaster (2001, 2002) used SVD analysis of observations to define the maximum covariability of spatial associations between the transition conditions in the MAM season with rainfall over the Indian region (5°–40°N, 60°–100°E) for the monsoon season of JJAS. For MAM, they used 1) observed 500-hPa height anomalies over Asia that, when positive, represent atmospheric circulation anomalies (e.g., warm air advection from the south) and associated anomalously warm Asian land temperatures with an enhanced meridional temperature gradient that could strengthen subsequent monsoon rainfall; 2) observed Indian Ocean SSTs that, if anomalously warm, could provide a moisture source for greater monsoon rainfall

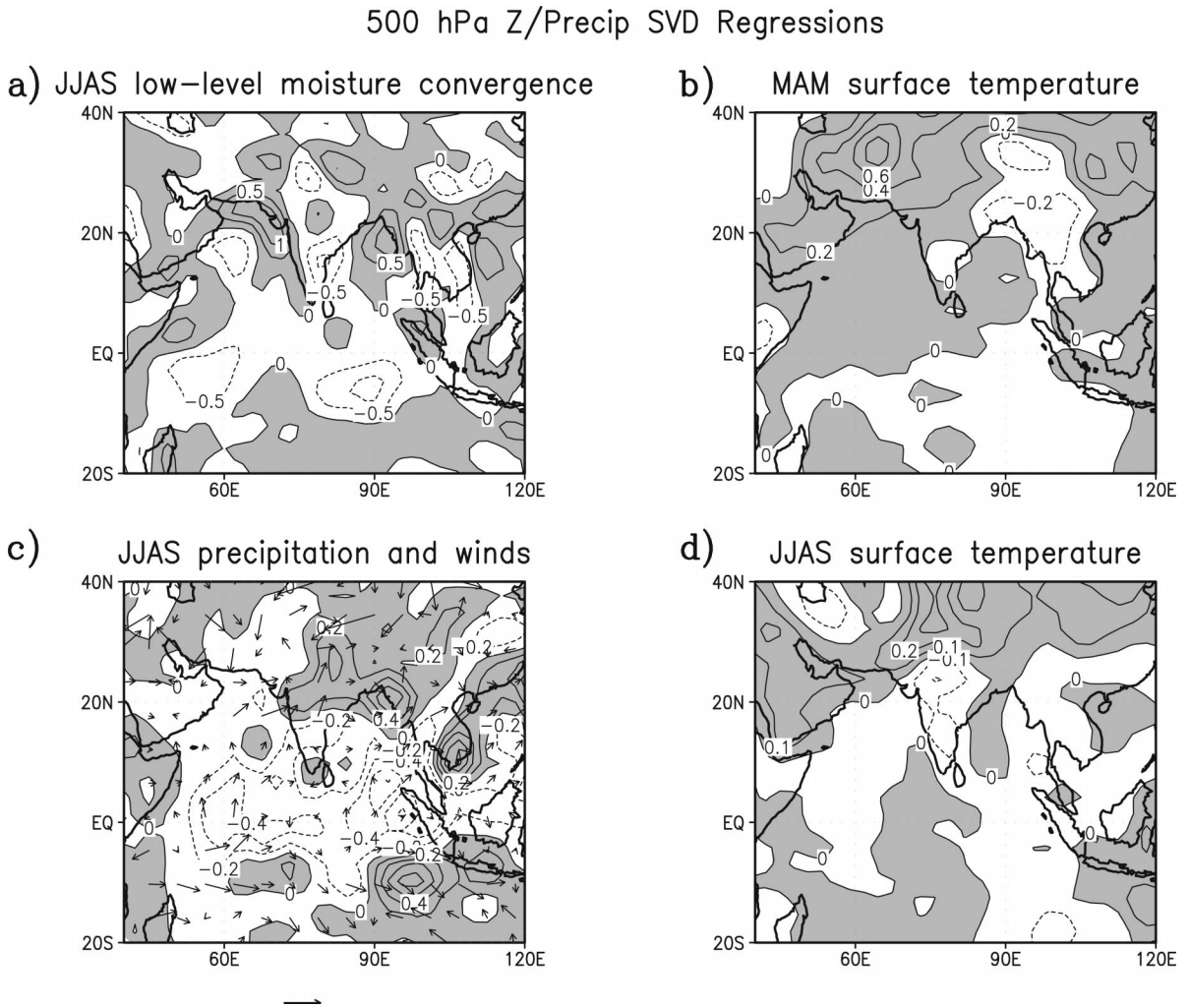

FIG. 2. The JJAS Indian monsoon precipitation SVD expansion coefficient time series derived from MAM 500-hPa height anomalies (Z) over Asia regressed against surface wind, precipitation, surface temperature, and low-level moisture convergence for seasons indicated. Units are m s^{-1}, mm day^{-1}, °C, and g kg^{-1} s^{-1} per unit std dev of the expansion coefficient of the first JJAS precipitation vector for surface wind, precipitation, surface temperature, and low-level moisture convergence, respectively. Scaling vector below (c) is 0.75 m s^{-1}. (a) Low-level moisture convergence for JJAS, (b) surface temperature for MAM prior to the Indian monsoon, (c) precipitation and surface winds for JJAS Indian monsoon season, and (d) surface temperature for JJAS Indian monsoon season.

through enhanced evaporation; and 3) observed eastern equatorial Pacific SSTs that could affect monsoon rainfall through changes in the large-scale atmospheric east–west circulation.

The time evolution of the conditions associated with the TBO can be constructed by regressing the SVD expansion coefficient time series computed for JJAS precipitation and MAM 500-hPa height, JJAS precipitation and MAM Indian Ocean SST, and JJAS precipitation and MAM Pacific Ocean SSTs against precipitation, surface wind and surface temperature data, and low-level moisture convergence (moisture convergence in the lowest model level). The JJAS Indian monsoon precipitation SVD expansion coefficient time series derived for MAM 500-hPa height anomalies over Asia regressed for MAM against surface temperature, and the MAM 500-hPa height expansion coefficient SVD time series regressed against JJAS surface wind, surface temperature, precipitation, and low-level moisture convergence is shown in Fig. 2 (the temperature and precipitation patterns in Figs. 2b and 2c, respectively, as in Meehl and Arblaster 2001, 2002). For MAM in Fig. 2b, there are warmer land temperatures (regression values greater than +0.3°C per unit standard deviation of the expansion coefficient of the first precipitation vector) over most of the areas north and west of India and east Asia, which is related to the enhanced meridional temperature gradient discussed by Meehl and Arblaster (2001, 2002). There is positive low-level moisture convergence in JJAS (Fig. 2a) over parts of northern India, Bay of Bengal, Bangladesh, and Burma (regression values of greater than +0.5 g kg^{-1} s^{-1} per unit standard

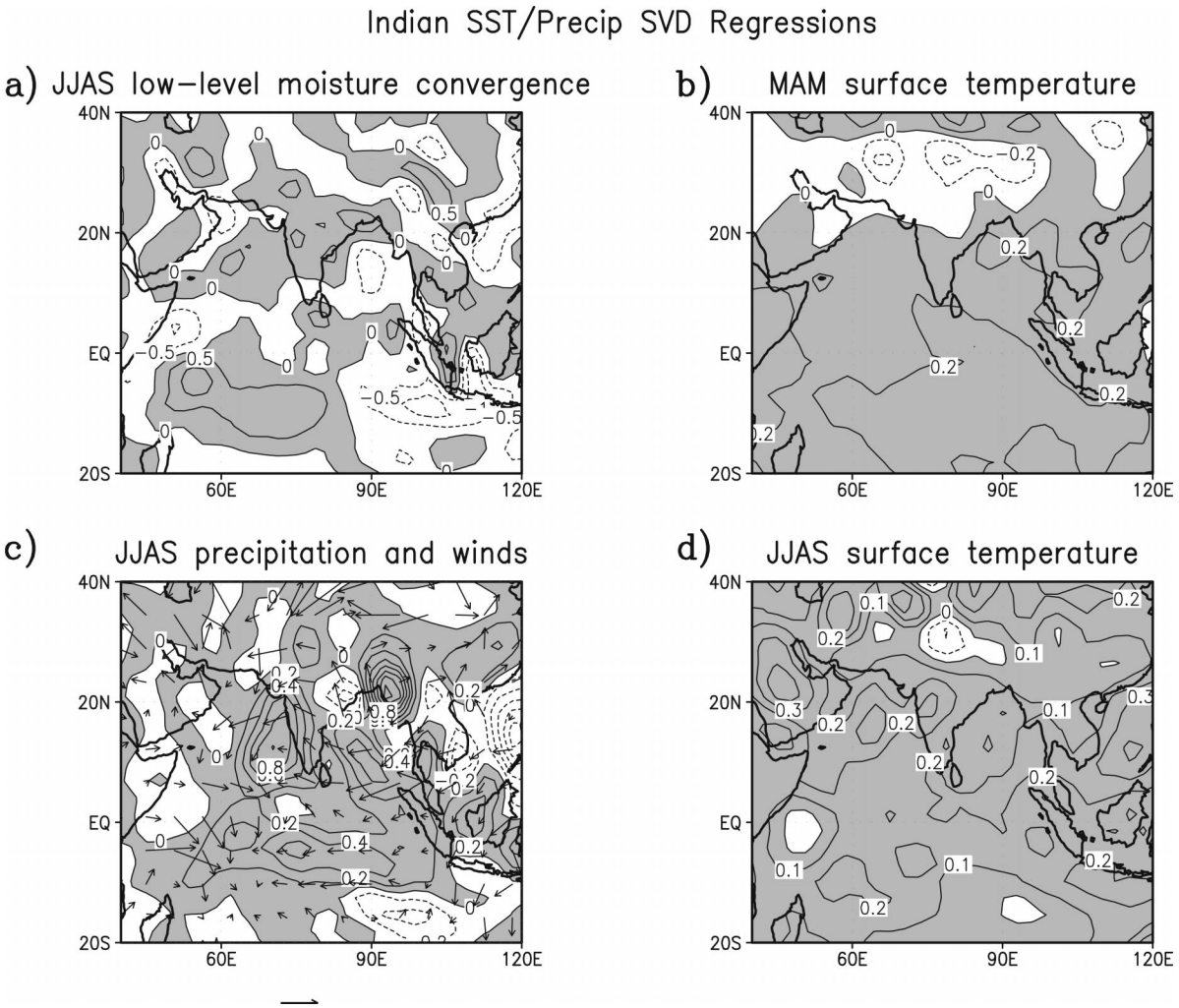

FIG. 3. The JJAS Indian monsoon precipitation SVD expansion coefficient time series derived from MAM Indian Ocean SST anomalies regressed against surface wind, precipitation, surface temperature, and low-level moisture convergence for seasons indicated. Units are m s^{-1}, mm day^{-1}, °C, and g kg^{-1} s^{-1} per unit std dev of the expansion coefficient of the first JJAS precipitation vector for surface wind, precipitation, surface temperature, and low-level moisture convergence, respectively. Scaling vector below (c) is 0.75 m s^{-1}. (a) Low-level moisture convergence for JJAS; (b) surface temperature for MAM prior to the Indian monsoon; (c) precipitation and surface winds for JJAS Indian monsoon season; (d) surface temperature for JJAS Indian monsoon season.

deviation of the expansion coefficient of the first precipitation vector), and moisture divergence over most of the equatorial Indian Ocean. The consequent precipitation patterns (Fig. 2c) follow areas of moisture convergence/divergence with positive regression values of several tenths of a mm day^{-1} over northeastern India and Bangladesh, and suppressed precipitation over the Indian Ocean north of about 5°S, and parts of eastern Asia, Malaysia, and Indonesia. The enhanced precipitation component has almost an ITCZ-like aspect with a band of positive precipitation regression values extending from India across the South China Sea and east of the Philippines as shown by Meehl and Arblaster (2001, 2002). There are strengthened south and southwest winds across the Arabian Sea with regression values of about 0.3 m s^{-1}. In Fig. 2d, SST regression values over the Indian Ocean are near zero.

Regressing the SVD expansion coefficient time series from the JJAS Indian monsoon rainfall calculated using the MAM Indian SST against surface winds, temperatures, precipitation, and low-level moisture convergence shows positive precipitation anomalies over most of India, Bangladesh, and the Indian Ocean (some regression values exceed +0.8 mm day^{-1}) in JJAS in Fig. 3c. Figure 3a shows enhanced low-level moisture convergence over most of these areas of positive rainfall with values over much of India of about +0.5 g kg^{-1} s^{-1}. The warm Indian Ocean SSTs in MAM (Fig. 3b) and JJAS (Fig. 3d) are associated with anomalous positive moisture convergence over most of the Indian Ocean

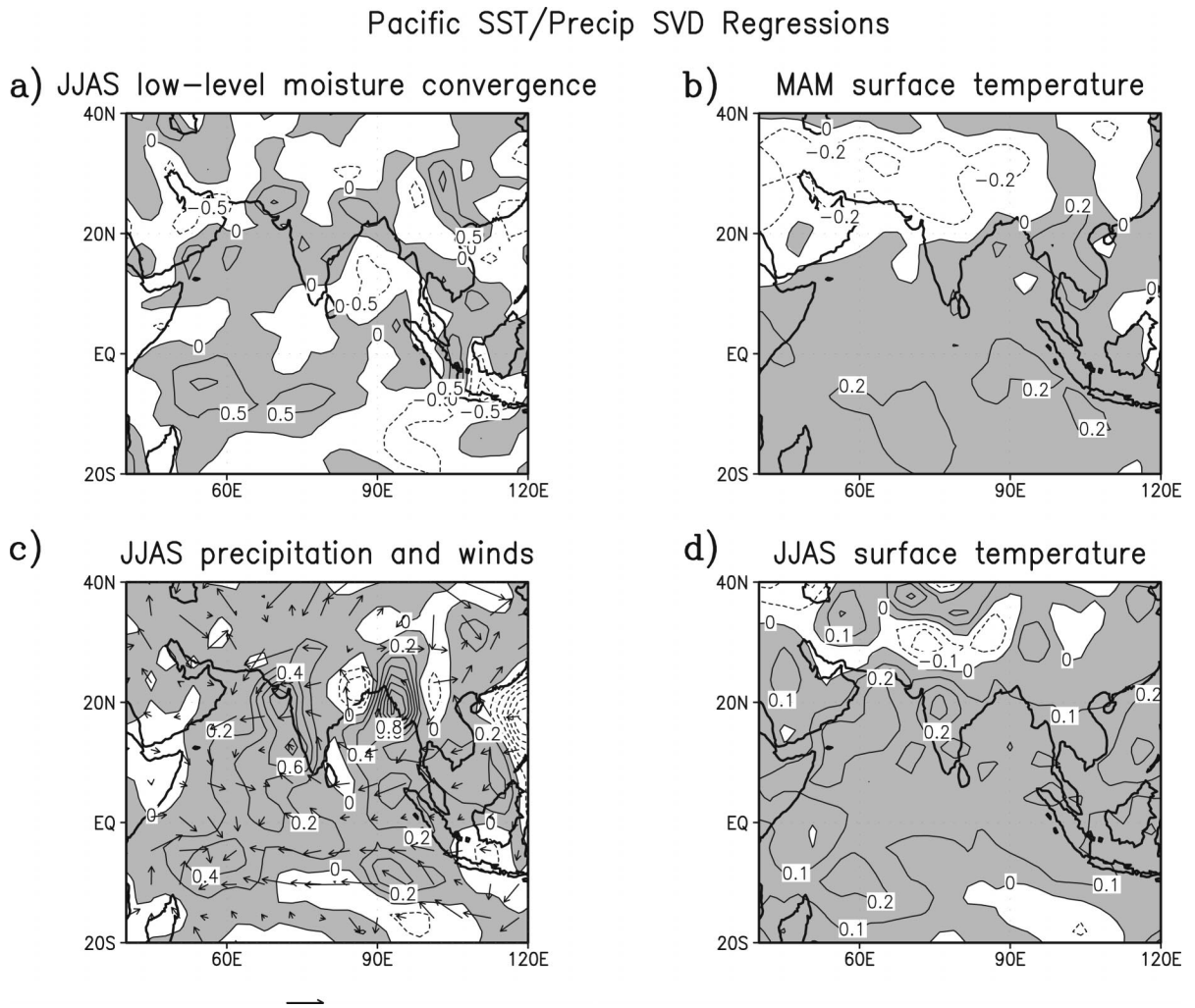

FIG. 4. The JJAS Indian monsoon precipitation SVD expansion coefficient time series derived from MAM Pacific Ocean SST anomalies regressed against surface wind, precipitation, surface temperature, and low-level moisture convergence for seasons indicated. Units are m s^{-1}, mm day^{-1}, °C, and g kg^{-1} sec^{-1} per unit std dev of the expansion coefficient of the first JJAS precipitation vector for surface wind, precipitation, surface temperature, and low-level moisture convergence, respectively. Scaling vector below (c) is 0.75 m s^{-1}. (a) Low-level moisture convergence for JJAS; (b) surface temperature for MAM prior to the Indian monsoon; (c) precipitation and surface winds for JJAS Indian monsoon season; (d) surface temperature for JJAS Indian monsoon season.

north of about 10°S (Fig. 3a), anomalous westerly surface wind regression values of about 0.4 m s^{-1} in the western equatorial Indian Ocean, and anomalous easterlies with regression values of around 0.5 m s^{-1} in the eastern Indian Ocean stretching across most of Southeast Asia (Fig. 3c). Small negative SST anomalies appear off the coast of equatorial Africa in the western Indian Ocean in JJAS (Fig. 3d).

A comparable calculation for Pacific SSTs and JJAS Indian monsoon rainfall (Fig. 4) shows similar patterns to that for the Indian SSTs in Fig. 3. Note that the sign convention here is for warm equatorial Pacific SSTs in MAM to transition to anomalously cool SSTs in JJAS as in Fig. 1, opposite to the sign convention in Meehl and Arblaster (2001, 2002). This is to facilitate comparison of the SVD patterns to the GCM sensitivity experiments to follow. The MAM SST regression values in the Arabian Sea and Bay of Bengal are near zero to +0.2°C for the Pacific SST regression in Fig. 4b compared to the Indian SST regression values in most areas of greater than +0.2°C in Fig. 3b. The small negative SST regression values in the western equatorial Indian Ocean in the Indian SST regression in Fig. 3d are not as obviously portrayed in the Pacific SST regression in Fig. 4d. Otherwise, the low-level moisture convergence, precipitation, and wind regression values are similar for the Indian and Pacific regression calculations in Figs. 3 and 4 indicating that their covariabilities are related in many years. Exactly in which years these are related is quantified below.

Meehl and Arblaster (2001, 2002) used the first SVD components for three separate conditions since those are

the dominant relationships accounting for a majority of the squared covariance (the first SVD components for the 500-hPa height, Indian SSTs, and Pacific SSTs accounted for 39%, 58%, and 39%, respectively, while the second SVD components for the three transition conditions accounted for 18%, 14%, and 19%, with the third through fifth components for all three accounting for considerably less). However, they noted that there clearly was no requirement that the first SVD components from the three transition conditions be orthogonal. In fact, they showed that the patterns of precipitation for Indian and Pacific SST transition conditions are closely related as noted above in Figs. 3 and 4.

Even though these conditions are related, there is a way to identify their relative contribution in a given monsoon season. Meehl and Arblaster (2001, 2002) calculated spatial anomaly pattern correlations between the observed JJAS rainfall patterns and the SVD projections individually (Fig. 5a) and cumulatively (Fig. 5b) using a variation of the technique of Lau and Wu (1999). A large positive correlation indicates a strong association with the observed monsoon rainfall pattern for that year. In this way it is possible to quantify the magnitude of the associations of the various transition conditions (either none, some, or all) in MAM with the subsequent JJAS monsoon rainfall year by year. We will refer to Fig. 5 later when we show case studies of individual years from observations to illustrate each of the transition conditions.

To return to the relationship between the tropical Pacific and Indian Ocean SST conditions, we note in Fig. 5a that the association between tropical Pacific and Indian SSTs and the pattern of Indian monsoon rainfall is large in some El Niño years (e.g., 1982) and La Niña years (e.g., 1988). Both have pattern correlation values greater than nearly +0.4 in Fig. 5a. In other years they act independently (e.g., 1992 and 1994). This demonstrates that in some years the Indian Ocean can provide a regional input to monsoon rainfall separate from large-scale influences emanating from the Pacific. Interestingly, the Indian and Pacific conditions follow each other fairly closely before about 1990, but less so after that. This likely relates to the sustained warm conditions in the Pacific in the early 1990s and the consequent effects in the Indian Ocean (Allan and D'Arrigo 1999).

In several years the regional 500-hPa/atmospheric circulation/Asian land/meridional temperature gradient condition is more dominant (e.g., 1980, 1990, 1993, 1995, and 1996) with correlation values above +0.4 in Fig. 5a. Connections between tropical Pacific SSTs, 500-hPa height, and Indian SST are strong in 1984, 1985, and 1989 when all have correlation values near to or greater than +0.4, thus confirming some of the studies cited earlier. In other years (1991, 1995, 1998) the three conditions are unrelated with widely different values. In 1984 when all three transition conditions have high correlation values (Fig. 5a), the cumulative value is about +0.8 (Fig. 5b) indicating over 60% of the spatial variance of the pattern of monsoon precipitation is accounted for in that year. However in 1986 when all of the three conditions are near zero for their individual associations in Fig. 5a, the cumulative pattern correlation in Fig. 5b is also near zero indicating other processes or internal dynamics are more important for the pattern of monsoon rainfall in that year. The point is

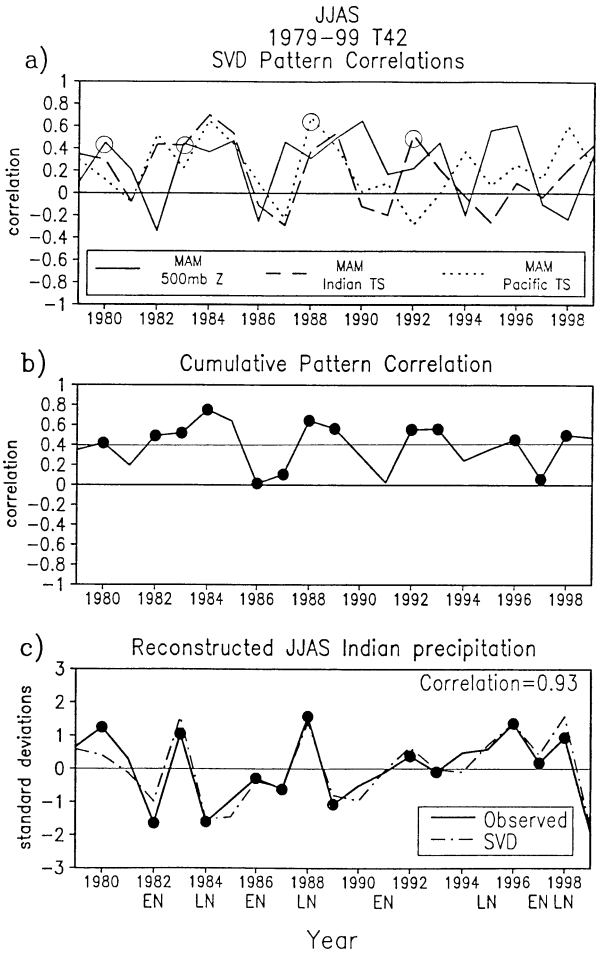

FIG. 5. (a) Time series, 1979–99, of individual anomaly pattern correlations for the regional (500-hPa height, Indian Ocean SST) and large-scale (Pacific surface temperatures) MAM SVD-derived conditions with observed JJAS Indian monsoon rainfall patterns for the area 5°–40°N, 60°–100°E. (b) Cumulative anomaly pattern correlations for Indian monsoon rainfall combining the three conditions in (a). The nominal significance level of 0.40 (marked in figure with thin solid line) is determined by a Monte Carlo technique described by Meehl and Arblaster (2001). (c) Time series of an index of Indian monsoon strength (area averaged over Indian region, all points, 5°–40°N, 60°–100°E) of the cumulative precipitation patterns in (b) derived from the SVD analysis normalized by their respective std dev (dash–dot line), and the full area-averaged normalized precipitation index over the same region calculated from the original precipitation data (solid line). El Niño (EN) and La Niña (LN) onset years are denoted beneath the corresponding years. Solid dots in (b) and (c) indicate relatively strong and weak monsoon years in relation to previous and following years for the observed index in (c). Large circles in (a) indicate years chosen for case studies. (After Meehl and Arblaster 2001.)

that in any given year, we quantify the magnitude of the associations of the various transition conditions (either none, some, or all) in MAM with the subsequent JJAS monsoon rainfall.

To relate the precipitation anomaly patterns to an area-averaged monsoon index and consequently the magnitude of the TBO, Meehl and Arblaster (2001, 2002) calculated regressions of the SVD expansion coefficient time series and the SVD rainfall patterns over the Indian region to produce a cumulative area-averaged Indian rainfall index (Fig. 5c). The correlation between the SVD-derived normalized cumulative index of monsoon ''strength'' and the full area-averaged normalized index (area averaged over Indian region, all points, 5°–40°N, 60°–100°E) from the original CMAP precipitation data is +0.93 (significant at greater than the 1% level) thus showing the SVD-derived index can capture 86% of the variance of the full index.

Meehl and Arblaster (2001, 2002) also defined TBO monsoon years as a monsoon index value greater than the previous or following year, or less than the previous or following year (Meehl 1987). These are denoted in Fig. 5c as the large dots. In Fig. 5b, 10 of these 13 TBO years have greater cumulative correlations than the nominal 1% significance value of 0.4 (see further discussion in Meehl and Arblaster 2001, 2002), indicating that the transition conditions in Figs. 3, 4, 5, and quantified in Fig. 5a are strongly associated with 77% of the years with TBO transitions. Later in this paper case studies from observations will be shown, and the years selected are denoted by large circles in Fig. 5a.

4. GCM experiments

A TBO flip-flop or transition of Indian monsoon rainfall is important not only for the south Asian monsoon but for the Australian monsoon as well (Meehl and Arblaster 2002). The transitions from MAM to JJAS, in association with SST anomaly transitions in the tropical Pacific at that time of year, set the sense of the large-scale east–west atmospheric circulation that has well-known seasonal persistence from the Indian to the Australian monsoon (Shukla and Paolino 1983; Meehl 1987). Area-averaged correlation of Australian monsoon precipitation lagging the Indian monsoon is +0.55 for this period (Meehl and Arblaster 2002). Therefore, Indian monsoon transitions are crucial to understanding the mechanisms of the TBO not only for the Indian monsoon but for the Australian monsoon as well. These transitions were shown by Meehl and Arblaster (2002) and noted earlier to be associated with various interrelated factors involved with the seasonal cycle of convection in the Asian–Australian monsoon, coupled SST anomalies in the tropical Indian and Pacific Oceans, associated surface wind anomalies in the Indian and western equatorial Pacific, and the consequent ocean dynamical response. We discussed above that these factors are not independent and it is possible to show their relative contributions year by year in Fig. 5. However, it is difficult to determine with those techniques whether the specific conditions individually could actually contribute to a TBO monsoon transition, or whether these conditions come out of the SVD analysis in an unphysical way. Thus GCM sensitivity experiments are ideal for focusing on the response to specific conditions individually.

The strategy for these experiments is to specify the three transition conditions separately in seasons leading up to the Indian monsoon. We will then compare the results from the GCM experiments with those from the SVD analyses in Figs. 3–5. A simple measure of the success of the GCM experiments will be to compute the monsoon area-average precipitation index and compare to the index reconstructed from the SVD analyses (Fig. 5c). However, information on the patterns of monsoon rainfall is also of interest from the GCM experiments, though systematic errors in the model simulation of monsoon rainfall must be taken into account. Therefore, general features of the simulated precipitation patterns from the sensitivity experiments in the context of the model climatology will be discussed in comparison to the observations.

To document systematic errors from the model climatology for the Indian monsoon compared to observations, the JJAS mean precipitation and surface winds for the CCM3 (Fig. 6a) are compared to the observed quantities from 1979–99 (Fig. 6b). The precipitation differences are shown in Fig. 6c. As has been noted previously (Meehl and Arblaster 1998), the CCM3 consistently produces too much precipitation (more than 6 mm day^{-1}) over the equatorial western Indian Ocean near 65°E and the east coast of India, with less than observed precipitation (3–6 mm day^{-1}) over parts of Bangladesh, Burma, and Indochina. The observed precipitation maximum at about 5°S over the Indian Ocean in Fig. 6b is shifted north to about 2°S in the model (Fig. 6a). Otherwise the model simulates a reasonable distribution of precipitation and surface winds over the rest of the Indian Ocean and south Asia. Low-level southeast trades in the southern Indian Ocean cross the equator to provide southwesterly inflow into the monsoon with rainfall maxima covering most of India, the Bay of Bengal, and the tropical Indian Ocean in the model as well as in the observations.

The version of CCM3 here is a somewhat updated version from that used in the monsoon intercomparison of Gadgil et al (1998), and is the version used in the intercomparison of Kang et al. (2001, manuscript submitted to *J. Climate*, hereafter KANG). The features noted in Fig. 6 were documented in the former, which placed the CCM3 errors in mean monsoon rainfall distribution in the context of its ability to simulate the amplitude of interannual Indian monsoon variability reasonably well. The CCM3 has a relatively small amplitude seasonal migration of the primary rainbelt over the Indian monsoon compared to other models. In the

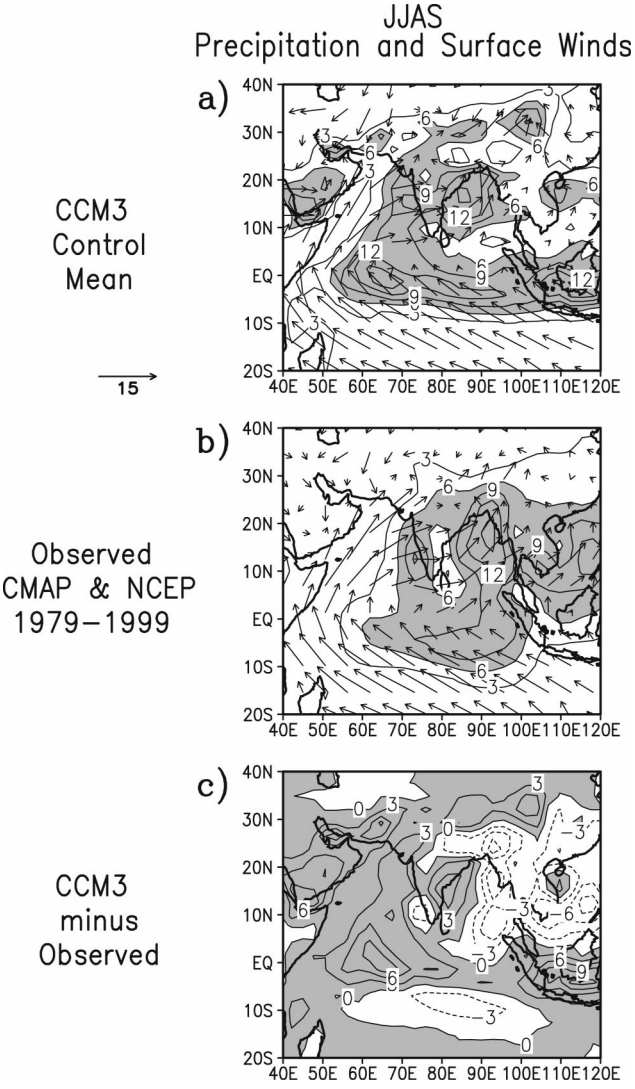

FIG. 6. (a) Seasonal mean JJAS rainfall (mm day^{-1}) over the Indian monsoon region from a 15-yr AMIP2 simulation with the NCAR CCM3. (b) Same as (a) except for observations, 1979–99. Scaling arrow is 15 m s^{-1} for (a) and (b). Contour interval is 3 mm day^{-1} with values greater than 6 mm day^{-1} shaded in (a) and (b). (c) Difference of model precipitation values in (a) minus observations in (b). Positive areas are shaded.

latter, the CCM3 did a comparable job to other models in simulating anomalies associated with the 1997/98 El Niño event.

We run the model with prescribed climatological SSTs to study the effects of the three Indian monsoon TBO transition conditions proposed earlier: anomalous Indian Ocean SSTs, anomalous Pacific SSTs, and enhanced meridional temperature gradients over Asia. Each experiment is initialized in January and run to October, with five-member ensembles started on different days in January to vary the initial conditions. The tropical Pacific SST anomalies were noted to change sign from MAM to JJAS in Fig. 1, with negative SST anomalies in JJAS associated with a strong monsoon. Thus in the experiments here with Pacific SST anomalies, they are specified to be negative for the duration of the experiment, with the caveat that, as shown by Meehl and Arblaster (2002), the association with the large-scale east–west atmospheric circulation is most important for the JJAS season between the Pacific SSTs and the Indian monsoon.

Anomalies are calculated from comparable integrations over the same time interval but with climatological conditions. Though various studies use either the JJA or JJAS average as the Indian monsoon season, here we use JJAS to be consistent with Meehl and Arblaster (2001, 2002) though we will mention results from JJA (which are nearly the same as for JJAS) for reference to other monsoon model intercomparisons (Gadgil et al. 1998; KANG) and previous studies with the CCM3 (Meehl and Arblaster 1998).

It was noted in Fig. 1 that in some years convective heating anomalies in DJF and MAM across the western Pacific–Indian Ocean region are associated with circulation and temperature anomalies over Asia that could influence the strength of the subsequent monsoon through anomalous meridional temperature gradients over Asia. Figure 2 showed that this influence is mostly manifested by enhanced monsoon precipitation over some south Asian land areas. To show the changes in observed meridional temperature gradient, the composite tropospheric temperature difference is averaged over 70°–90°E where this effect is most strongly seen at the surface (e.g., Fig. 2b) for positive minus negative values of the SVD expansion coefficient time series for the 500-hPa MAM heights covarying with JJAS monsoon rainfall. It can be seen in Fig. 7a that positive temperature anomalies extend from the surface through the depth of the troposphere north of about 25°N over Asia, thus enhancing the meridional temperature gradient from the Indian Ocean to northern Asia. Observed positive minus negative amplitudes in Fig. 7a range from nearly +1°C near 45°–50°N to almost −0.5°C near 15°–20°N for a north–south enhancement of about 1.5°C.

To induce such an effect in the model, we multiply surface albedo by 0.5 over a region of Asia encompassing 35°–70°N and 60°–120°E. This reduction in albedo has the effect of increasing absorbed solar radiation and warming not only the surface, but raising temperatures through the depth of the troposphere as shown in Fig. 7b. This is accomplished through enhanced sensible heat flux and subsequent mixing of the warmer surface air in the vertical (not shown) in association with a consequent anomalous 500-hPa ridge of positive heights with anomalies up to 45 m (not shown). The resulting increased meridional temperature gradient is set up a bit farther south than observed in Fig. 7a, but with comparable intensification. For the model the temperature differences in Fig. 7b range from over +1.5°C near 35°–50°N to slightly negative over the ocean for a north–south enhancement of greater than 1.5°C and

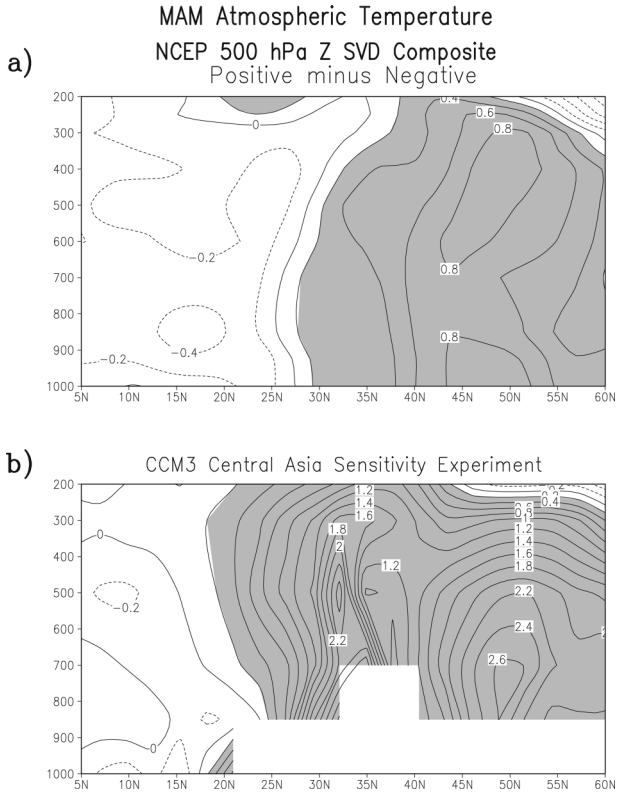

FIG. 7. (a) Zonal mean composite tropospheric temperature differences averaged over 70°–90°E for positive minus negative years in the expansion coefficient time series for the first SVD component of MAM 500-hPa height anomalies over Asia and JJAS Indian monsoon rainfall. Changes are evident in meridional temperature gradient, and differences greater than +0.2°C are shaded. (b) Same as (a) except for GCM experiment ensemble mean minus control, with specified lower surface albedo and consequent warm surface temperatures over Asia. Differences greater than +0.2°C are shaded.

up to 2.5°C. Therefore, this induced anomalous meridional temperature gradient is larger than observed and should be of sufficient magnitude to examine the model response independent from other forcings.

Figure 8a shows the five-member ensemble average anomalies of precipitation and surface vector wind for the meridional temperature gradient experiment. The shading indicates differences significant at greater than the 5% level. As in the observations (Fig. 2c), there is significantly enhanced rainfall (anomalies greater than +1.0 mm day^{-1}) across north and northeast India extending into Burma and Thailand with weak southerly anomaly winds over the Indian Ocean from about the equator to near 15°N of about +0.5 m s^{-1} (Fig. 8a). There are also positive precipitation anomalies greater than +1.0 mm day^{-1} to the east over Vietnam and the South China Sea as seen in Fig. 8a, indicative of the enhanced ITCZ-type pattern discussed earlier. In the context of the model climatology in Fig. 6a, the positive differences across northern and northeastern India and parts of Burma are in situ enhancements of the climatological precipitation maxima. Comparing the corresponding SVD precipitation pattern in Fig. 2c to the observed climatology in Fig. 6b, the positive differences in northern India and the Bay of Bengal and Burma are also in situ enhancements of climatological precipitation maxima.

Computing a normalized area-averaged JJAS Indian monsoon precipitation index for these experiments gives a value of +0.78 standard deviations that indicates a slight strengthening of the monsoon. If the JJA season is used, the area-averaged index increases to +1.3 standard deviations. In any case, this experiment shows that an enhanced meridional tropospheric temperature gradient by itself can somewhat enhance monsoon precipitation over south Asian land areas as suggested by the SVD analyses of observations. That this is a weak response is indicated by Fig. 7 where the specified strengthened meridional temperature gradient was noted earlier to be almost twice that in the observations.

In Fig. 9a we show low-level moisture convergence anomalies for the Asian land temperature increase experiment, and latent heat flux anomalies are shown in Fig. 10a. There are statistically significant (shaded areas indicate 5% significance) positive values of moisture convergence of around 2 g kg^{-1} s^{-1} coinciding with the statistically significant increases of precipitation over northeast India and Burma (Fig. 8a). Since SSTs in the Indian Ocean do not change, the statistically significant increases of latent heat flux of around 10 W m^{-2} in Fig. 10a are due mostly to changes of wind speed induced by the warmer Asian land temperatures. Low-level moisture convergence then fuels the increases of precipitation over south Asian land areas. The moister land surfaces there then produce increases of latent heat flux in Fig. 10a.

To test the effect of warmer Indian Ocean SSTs on the monsoon, we increase SSTs by 0.75°C north of 15°S. This can be compared to maximum observed positive minus negative TBO year composite values calculated by Meehl et al. (2002, manuscript submitted to *J. Climate*, hereafter MAL) in DJF and MAM, respectively, of about +0.6°C, thus giving the model a somewhat larger forcing than observed. Results from this experiment for a five-member ensemble in Fig. 8b show enhanced precipitation significant at greater than the 5% level over most Indian Ocean areas (positive anomalies of +2 to +6 mm day^{-1}). There are westerly anomaly winds from about +1 to +2 m s^{-1} over much of the equatorial Indian Ocean as noted for the observations in Fig. 3c. There are also statistically significant positive precipitation anomalies of about +1 to +3 mm day^{-1} over much of western, northern, and northeastern India. In the context of the model climatology in Fig. 6a, the positive values in the model experiment in Fig. 8b, appearing as bands near 5°N and 5°–10°S over the Indian Ocean, are expansions of the climatological precipitation maximum band near 2°S. Over the Bay of Bengal, the model's climatological maximum is modified with positive anomalies to the north over northeastern India

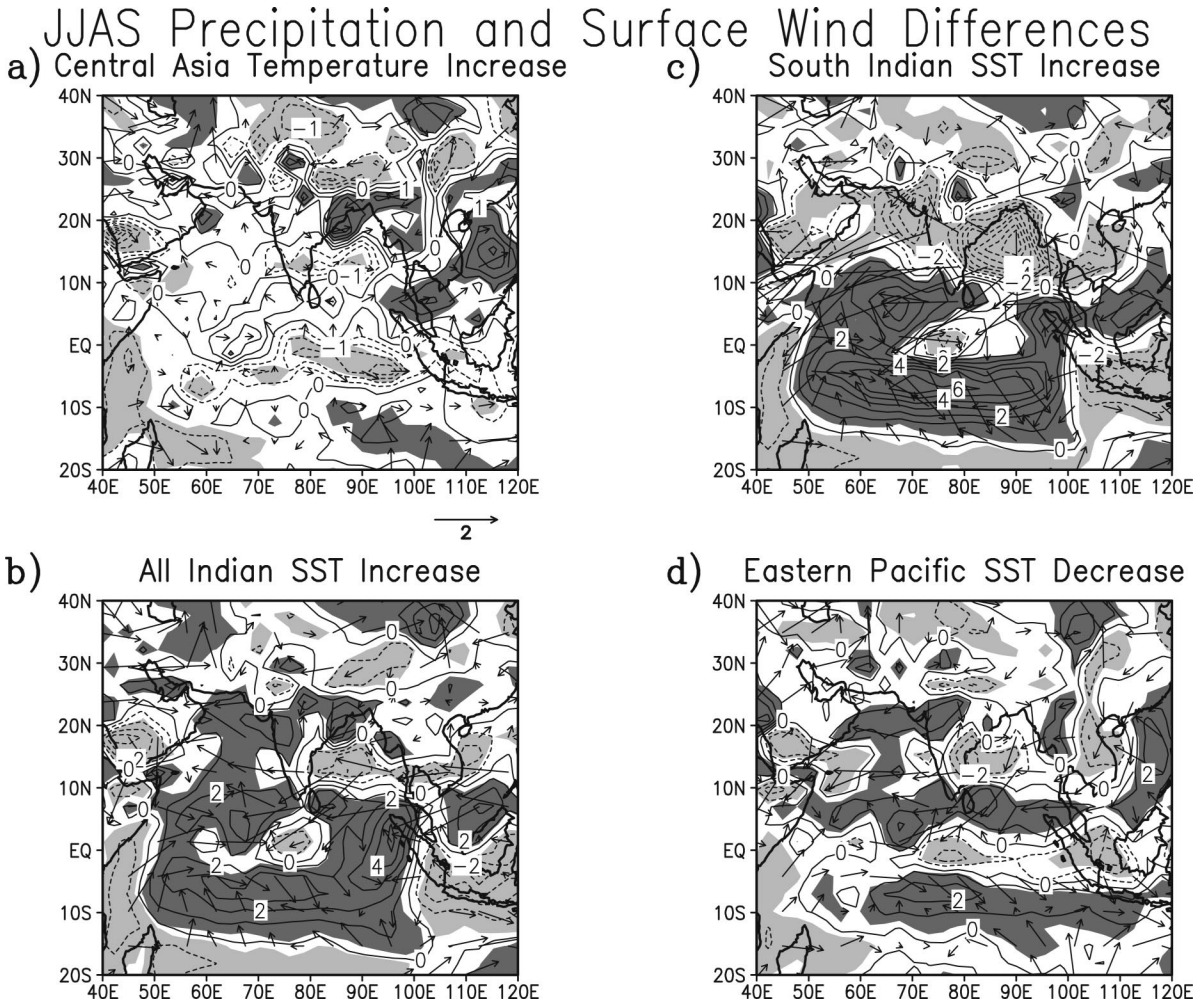

FIG. 8. Five-member ensemble mean averages minus control for JJAS precipitation (mm day^{-1}) and surface wind [scaling vector below (a) in m s^{-1}]. (a) Central Asia surface temperature increase experiment, (b) experiment with Indian Ocean SSTs increased by 0.75°C north of 15°S, (c) experiment with Indian Ocean SSTs increased by 0.75°C from 15°S–10°N, and (d) experiment with Pacific Ocean SSTs decreased by 2.0°C over the area 10°S–10°N, 175°E–80°W. Contour interval is 1 mm day^{-1}. Shading denotes areas significant at the 5% level, dark shading for positive anomalies, light shading for negative.

and to the south near 5°S. The model climatological precipitation is enhanced in situ over northwestern India in the sensitivity experiment (Fig. 8b). For the observations, the climatological precipitation maximum band near 5°S is shifted north in the SVD analysis in Fig. 3c, while the climatological precipitation maximum off the west coast of India is intensified in situ in Fig. 3c. The model has no precipitation maximum in the latter location in the climatology in Fig. 6a, so there is no evidence of any significant precipitation increase in the sensitivity experiment in that location (Fig. 8b).

Thus, though the patterns of anomalous precipitation in the observations in Fig. 3c and the model sensitivity experiment in Fig. 8b do not correspond exactly, they can be understood in terms of the respective climatologies, with significantly increased precipitation over much of the monsoon region. This is demonstrated by computing the change of the normalized area-averaged JJAS Indian monsoon precipitation index (area averaged over the Indian region, all points, 5°–40°N, 60°–100°E). For the model experiment in Fig. 8b it is +3.50 standard deviations (the JJA value increases +5.1 standard deviations) indicating that anomalously warm Indian Ocean SSTs can, by themselves, strengthen the regional Indian monsoon. The fact that this occurs mainly through an enhanced low-level moisture source is indicated in Fig. 9b. There are statistically significant positive surface moisture convergence anomalies for JJAS of +2 to +4 g kg^{-1} s^{-1} over areas of India and the tropical Indian Ocean where precipitation is greater in Fig. 8b. The increased moisture source from evaporation is shown by the large statistically significant increases of latent heat flux (greater than 20 W m^{-2}) over the southern and western Indian Ocean and the Bay of Ben-

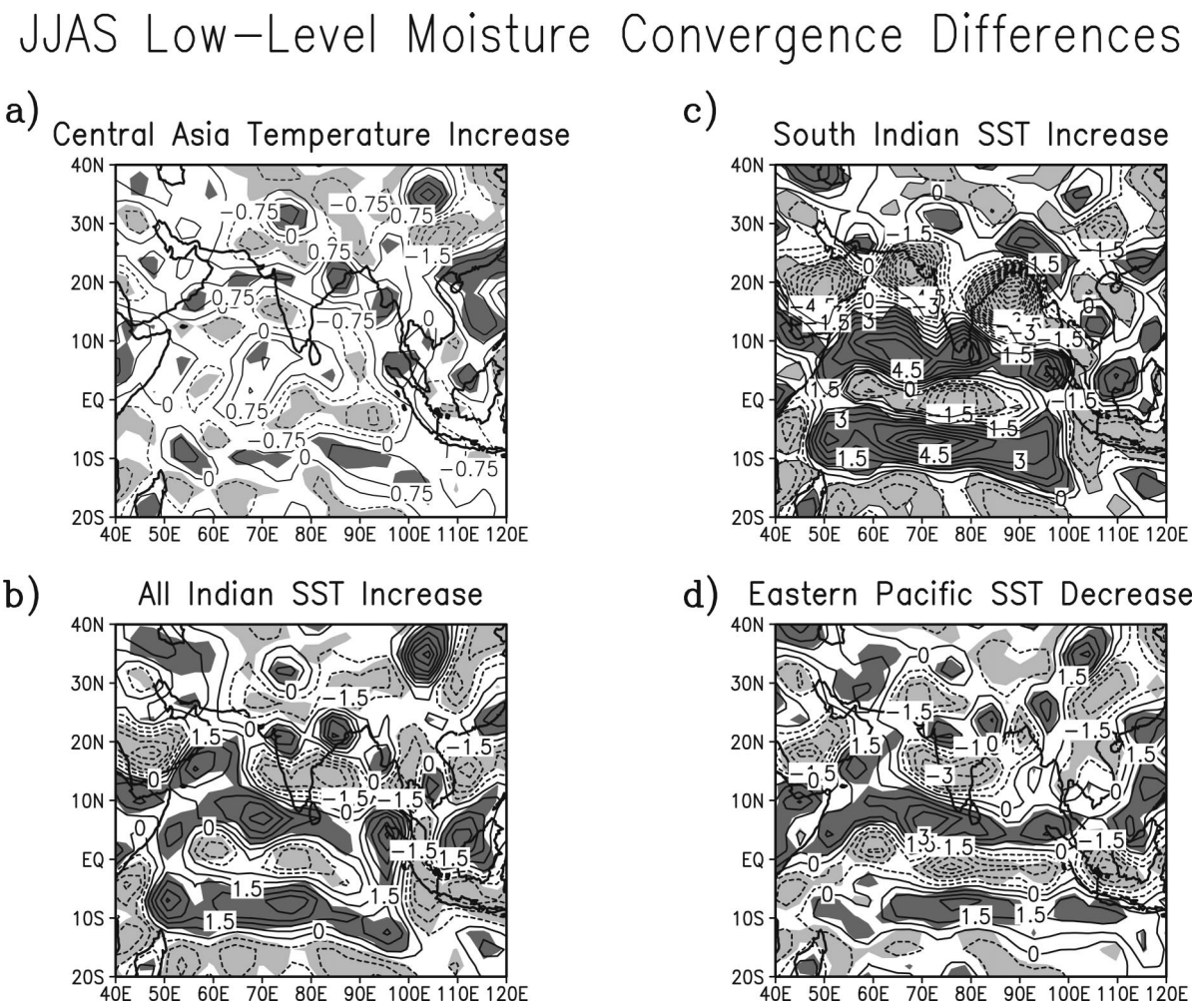

FIG. 9. Same as Fig. 8 except for low-level moisture convergence anomalies (contour interval is 0.75 g kg^{-1} s^{-1}).

gal. This increased moisture source, more than double that seen for the warm Asian land experiment in Fig. 10a, contributes to the enhanced moisture convergence and stronger precipitation in Figs. 9b and 8b, respectively.

In Fig. 3c the anomalous winds over the Arabian Sea are easterly in the observations, which is somewhat counterintuitive for a ''strong'' monsoon that is often thought of in terms of larger-amplitude southwesterlies over the Arabian Sea. In fact the model experiment in Fig. 8b shows easterly anomaly winds across the southern Bay of Bengal and eastern and northern Arabian Sea of 1–2 m s^{-1} in association with enhanced monsoon precipitation over most of India (Fig. 8b). This is due to the proportionately larger areas of precipitation increase over the Indian Ocean compared to south Asian land, lower sea level pressure over the warmer ocean (not shown), and a consequent anomalous cyclonic circulation north of the equator in the Indian region.

Studies cited previously indicated that warmer SSTs in some areas of the tropical Indian Ocean south of India could produce decreased monsoon rainfall over south Asian land areas (Yamazaki 1988; Chandrasekar and Kitoh 1998). To investigate this further, we performed another experiment where we increased SSTs by 0.75°C over the Indian Ocean only from 15°S to 10°N. This is also more comparable to the pattern associated with non-ENSO onset years from the SVD analyses in Meehl and Arblaster (2002, their Fig. 11c). Results from a five-member ensemble in Fig. 8c show statistically significant positive precipitation anomalies greater than +4 mm day^{-1} over the Indian Ocean with only a few small areas of positive values greater than +1 mm day^{-1} over central India and Burma. There are mostly statistically significant negative values over India greater than −2 mm day^{-1}. The change of the normalized area-averaged JJAS Indian monsoon precipitation index for the model experiment in Fig. 8c is −1.10 standard deviations.

There are also westerly anomaly winds of greater than +2 m s^{-1} over the western equatorial Indian Ocean as

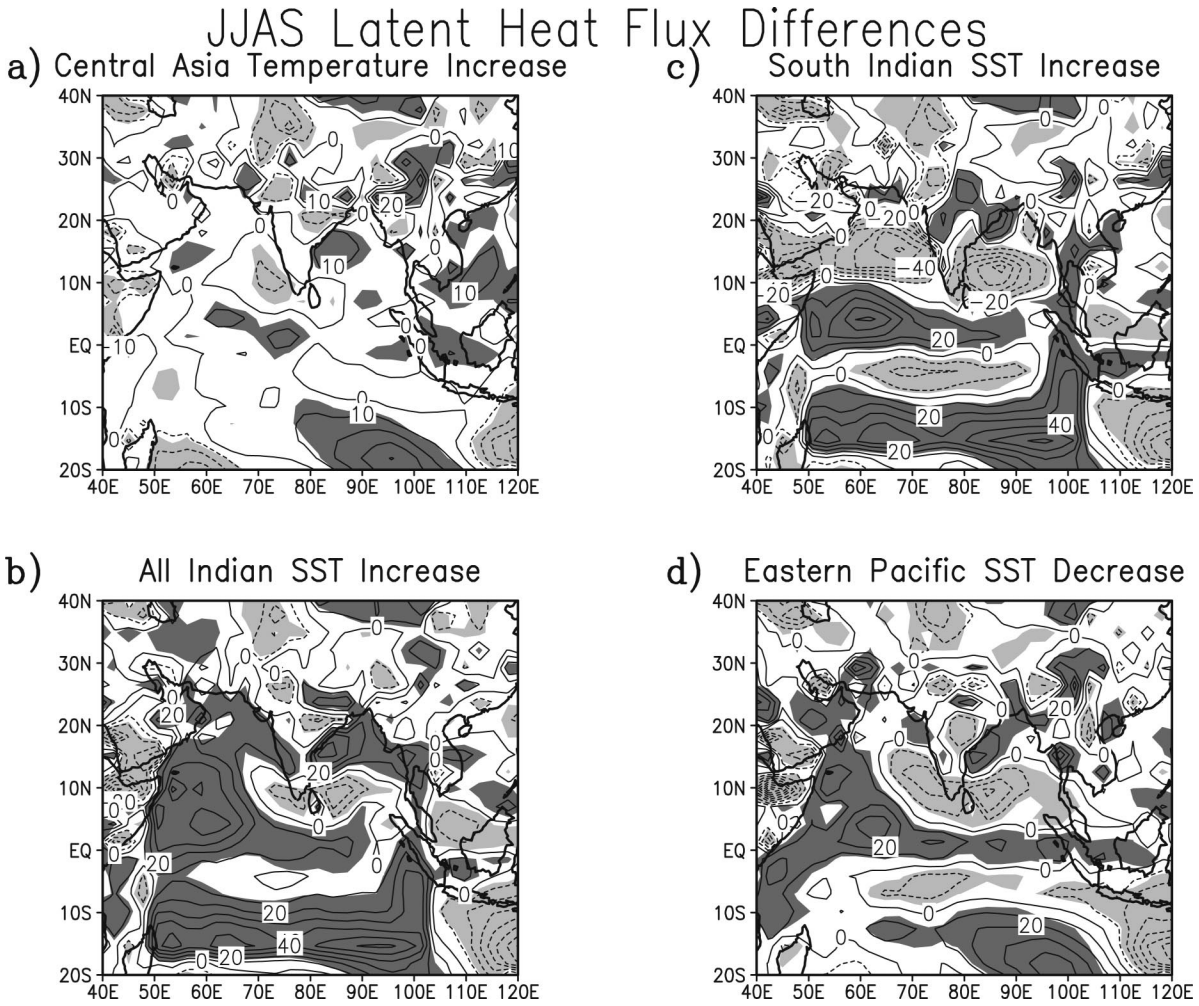

FIG. 10. Same as Fig. 8 except for latent heat flux anomalies (W m^{-2}). Positive values indicate heat lost from the surface.

in Fig. 8b, but easterly anomalies of that size over the Arabian Sea. This confirms the earlier model results cited above in that warm SST anomalies south of India cause a local enhancement of precipitation with mostly decreases over south Asian land areas. Maximum decreases are the result of a suppression of the climatological maxima of precipitation over northwest India and the Bay of Bengal (Fig. 6a), while the increases over the Indian Ocean resemble those in Fig. 8b with a spreading of the southern precipitation maximum band resulting in two bands of positive precipitation anomalies near 5°N and 5°–10°S.

Additionally, the easterly anomaly winds over parts of the Arabian Sea, India, and Bay of Bengal in both Figs. 8b and 8c show that the monsoon system is dynamically feeling the influence of the anomalously warm SSTs in the Indian Ocean with corresponding lower sea level pressure north of the equator and anomalous cyclonic flow with consequent easterly anomaly surface winds. Statistically significant positive moisture convergence anomalies in Fig. 9c of up to +4 g kg^{-1} s^{-1} and mostly positive latent heat flux anomalies in Fig. 10c greater than +20 W m^{-2} south of 10°N over the areas of increased SSTs indicate the local nature of the moisture source for the precipitation anomalies in Fig. 8c. Thus the Arabian Sea low-level inflow can be affected by numerous factors, not simply the amount of precipitation over land areas of India.

Figure 1 conceptually shows what was quantified in Figs. 3 and 4 that warm Indian Ocean SSTs and cool Pacific SSTs in JJAS are often associated with greater monsoon rainfall across most areas of south Asia and the Indian Ocean. The Indian Ocean SST experiments above show that the regional warming of SSTs there can produce enhanced monsoon rainfall. Yet, the question remains concerning the role of the large-scale effects from the Pacific SST anomalies. It is well known that relatively cool Pacific SSTs in JJAS are often associated with above-normal monsoon rainfall (Rasmusson and Carpenter 1983; Meehl 1987). To isolate the large-scale influence of anomalous tropical Pacific SSTs on the monsoon, we decrease SSTs by 2.0°C over the

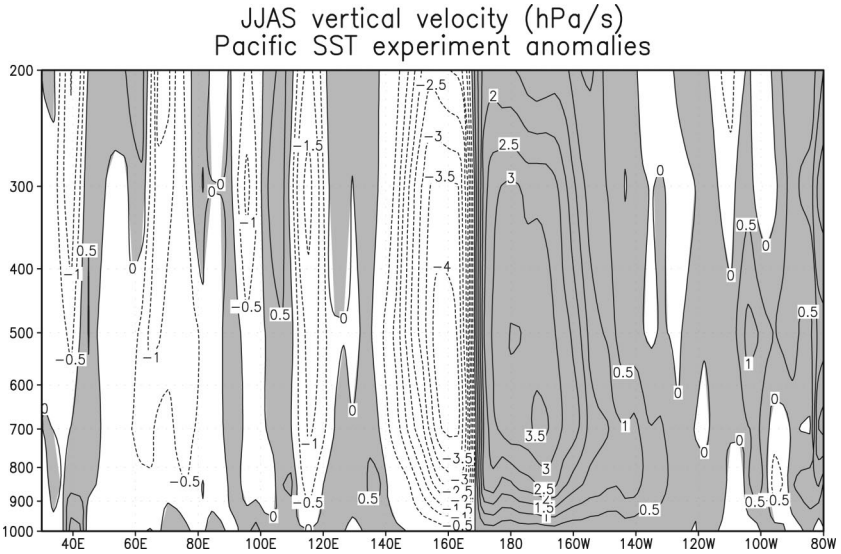

FIG. 11. Vertical velocity (omega) anomalies in JJAS averaged from 10°S–25°N for experiment with Pacific Ocean SSTs decreased by 2.0°C over the area 10°S–10°N, 175°E–80°W (hPa s^{-1}). Shading indicates positive (downward) motion.

area 10°S–10°N, 175°E–80°W. This SST anomaly compares to maximum values for JJAS in the TBO positive minus negative composites in MAL of about −1.5°C, thus again giving the model a somewhat larger-amplitude forcing compared to observations. The model response for a five-member ensemble in Fig. 8d shows statistically significant enhanced monsoon precipitation (anomalies around +2 mm day^{-1}) over parts of the northern Arabian Sea and tropical Indian Ocean, northwest India, and Burma. There are also areas of significant rainfall reduction over eastern India and the Bay of Bengal. The patterns in Figs. 8b from the Indian Ocean SST increase and Fig. 8d for the eastern Pacific SST decrease are similar in some respects. In terms of the model climatology, both have an expanded precipitation maximum south of India as indicated by bands of positive anomalies near 5°N and 5°–10°S. However, in Fig. 8d the expansion of the precipitation maximum to the east near western Sumatra is absent for the Pacific SST case in Fig. 8d. Both have an increase of the precipitation maximum over northwest India. But the climatological maximum over the Bay of Bengal in the model climatology in Fig. 6a, which was strengthened and shifted a bit north in the Indian SST case in Fig. 8b, is virtually unchanged in the Pacific SST case in Fig. 8d. Additionally, the overall regional strengthening of monsoon precipitation in Fig. 8b appears to be less in Fig. 8d. Indeed, the normalized JJAS monsoon index in Fig. 8d shows an increase of +1.7 standard deviations compared to +3.5 standard deviations in Fig. 8b for the Indian SST case (the JJA value increases +5.1 standard deviations for the Indian SST case in Fig. 8b compared to +3.3 standard deviations for the Pacific SST case in Fig. 8d). These results show that tropical Pacific SST anomalies can, by themselves, significantly strengthen monsoon precipitation, though not as significantly as Indian Ocean SST anomalies.

In the Pacific SST case in Fig. 8d the Indian Ocean SSTs do not increase. Thus the mechanism producing the monsoon rainfall anomalies in Fig. 8d must be related to remotely forced circulation anomalies. These are associated with the statistically significant changes in low-level moisture convergence in Fig. 9d and latent heat flux in Fig. 10d and involve the well-known linkage via the large-scale east–west atmospheric circulation. To illustrate this, Fig. 11 shows vertical velocity (omega) anomalies averaged from 10°S to 25°N across the Indian and Pacific regions. Anomalous upward (negative) vertical velocity anomalies predominate in the Indian region from about 50° to 100°E where area-averaged increases of Indian monsoon precipitation were noted to occur above. Greatest increases of precipitation between 10°S and 25°N around 70°E, with values greater than +2 mm day^{-1} in Fig. 8d (near 20°, 5°N, and 7°S), are associated with largest midtropospheric values of enhanced upward vertical velocity differences greater than −1.5 hPa s^{-1} in Fig. 11. Anomalous downward (positive) anomalies lie in the region of the specified negative SST anomalies (and suppressed precipitation, not shown) east of 170°E. Strongest vertical velocity anomalies occur closest to the western part of the cool SST anomaly in the Pacific. The large amplitude negative anomalies near 160°E also occur in conjunction with increased precipitation there (not shown). The significant enhancement of precipitation associated with the negative vertical velocity anomalies from 100° to 120°E in Fig. 11 occurs mainly in the South China Sea and southern Indonesia in Fig. 8d. Since a uniform −2°C anomaly is superimposed on base-state SSTs that increase toward the west, the largest relative decreases in

evaporation in the sensitivity experiment occur where base-state SSTs are highest due to the Clausius–Clapeyron relationship between about 170°E and 160°W (not shown), corresponding to the largest decreases in precipitation and vertical velocity in Fig. 11. Thus, anomalous large-scale sinking in the region of the negative SST anomalies in the equatorial Pacific results in anomalous rising motion over the south Asian monsoon region. This produces changes to the low-level winds and areas of increased moisture convergence (Fig. 9d), associated increases in latent heat flux (Fig. 10d), and positive precipitation anomalies (Fig. 8d) in that region. Interestingly, as noted above, the pattern of precipitation response from local forcing due to anomalously warm Indian Ocean SSTs is similar in some ways to that from the remotely forced circulation response from the Pacific. Both forcings perturb the climatological pattern of precipitation south of India and over northwest India in similar ways, but produce different responses over the Bay of Bengal and near western Sumatra.

Figure 5a shows that the transition conditions often act in unison (i.e., all three are positive and account cumulatively for a significant part of the monsoon rainfall pattern, e.g., 1980, 1983, 1984, 1985, 1988, 1989, 1993, 1996, 1999), but in some years they act in opposition. For example, in 1992 there are positive contributions from the Indian SSTs and 500-hPa condition and negative for the Pacific SSTs. As will be shown later, most of the Indian Ocean SST forcing is centered south of India, which would produce a negative precipitation anomaly over the Arabian Sea, the Bay of Bengal, and northern India (Fig. 8c). However, there is a positive 500-hPa contribution in 1992 in Fig. 5a, a significant cumulative pattern correlation in Fig. 5b, and a positive area-averaged monsoon precipitation anomaly in Fig. 5c. Additionally, in 1982 and 1998 both SST single pattern correlation conditions in the Indian and Pacific are positive and acting to oppose the 500-hPa pattern correlation conditions that are negative. In those years the cumulative anomaly pattern correlation accounts for a significant portion of the actual monsoon precipitation in Fig. 5b, with values of about +0.5. Conversely, in 1987, 1990, and 1995, there is a large positive single pattern correlation contribution from the 500-hPa condition in Fig. 5a with mostly negative single pattern correlation contributions from the Indian and Pacific SST conditions. In both those years the cumulative anomaly pattern correlation in Fig. 5b is not significant. This suggests that the SST conditions may be more dominant contributors to anomalous monsoon rainfall compared to the 500-hPa condition.

To test how regional and large-scale forcings can combine to produce various monsoon precipitation anomalies, additional model sensitivity experiments are performed. A warming of the south Indian Ocean was seen to produce local increases of precipitation but *decreases* over the Arabian Sea, the Bay of Bengal, and India (Fig. 8c). An increase of central Asian temperatures produces *increases* of precipitation over some of those same regions of northern and eastern India. To examine the combined effects of a warming of central Asia and a warming of the southern Indian Ocean, five-member ensembles were performed with a combination of warm central Asia and warm south Indian Ocean, and the warm south Indian Ocean ensemble mean differences are subtracted from those ensemble differences and shown in Fig. 12a. Any significant differences that coincide with those in Fig. 8a indicate the contribution of those precipitation anomalies from warm Asian land temperatures that are able to arise in spite of being combined with the warm south Indian SSTs. Significant dif-

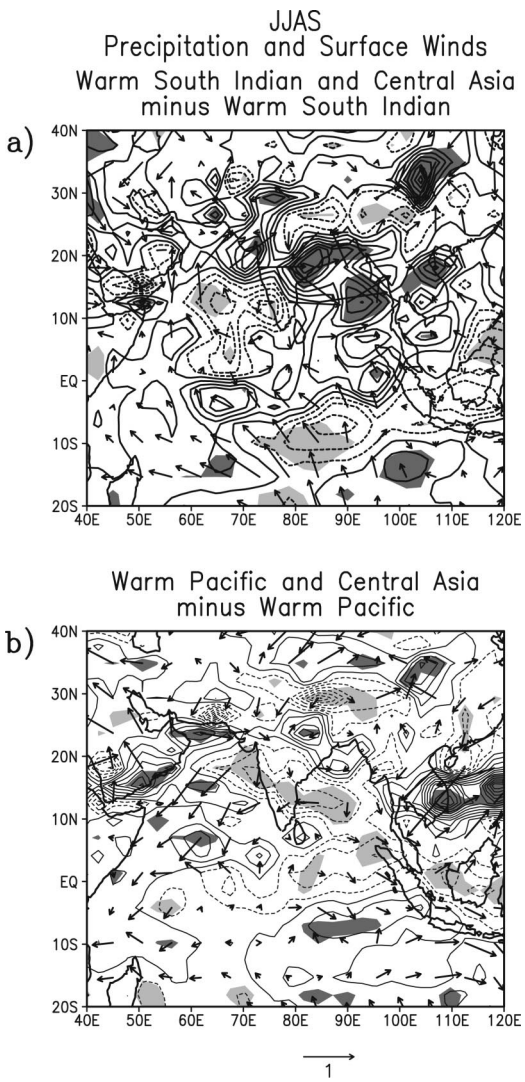

FIG. 12. (a) Precipitation differences of warm central Asia and warm south Indian Ocean combination ensemble anomalies minus the warm south Indian Ocean experiment ensemble anomalies (contour interval is 0.3 mm day^{-1}). (b) Precipitation differences of the warm Pacific and central Asia combination ensemble anomalies minus the warm Pacific experiment ensemble anomalies (contour interval is 0.3 mm day^{-1}). Shading indicates areas of 10% significance for 10 degrees of freedom.

ferences occur over northwest and northeast India extending into Burma and northern Thailand, Vietnam, and Laos in Fig. 12a. These significant increases of precipitation are in similar regions to those noted for the central Asian temperature increase experiment in Fig. 8a. Therefore, regional forcings acting in unison can produce changes in regional precipitation, with the effects of the central Asian temperature increase able to produce positive precipitation anomalies in areas where forcing from an anomalously warm southern Indian SST would produce negative precipitation anomalies. In this case the effects from the forcings are cumulative, with evidence of each forcing appearing in the experiment with both acting simultaneously.

The all–Indian Ocean SST experiment produced increases of precipitation over most of the same areas of northern and eastern Indian and Bangladesh as the central Asian temperature increase (cf. Figs. 8a and 8b). An ensemble of five experiments with the tropical Pacific SSTs anomalously warm by +2°C produced roughly an opposite pattern of precipitation over the Indian region as in Fig. 8d, with statistically significant decreases over large areas of the Indian Ocean and India itself (not shown). To examine the response when Pacific SSTs act in opposition to central Asian land temperatures produced by anomalous 500-hPa circulation, an ensemble of five experiments were performed combining warm Asian land temperatures as in Fig. 8a with warm Pacific SSTs (opposite to Fig. 8d). Thus, the warm Asian land temperatures would tend to increase precipitation over northern India, and the warm Pacific SSTs would tend to decrease precipitation over most of the monsoon region. Figure 12b shows the differences of the warm Pacific and central Asia combination ensemble anomalies minus the warm Pacific experiment ensemble anomalies. There is some evidence of the enhanced ITCZ influence of the warm Asian land temperatures noted in Fig. 8a, with positive precipitation differences over parts of the northern Arabian Sea, northern India, the Bay of Bengal, Vietnam, and the South China Sea. However, these differences are small and mostly not statistically significant. The large-scale influence from the tropical Pacific is more effective than the regional forcing from Asian land temperatures. Thus, in Fig. 5a in years when tropical Pacific SSTs work in opposition to the 500-hPa/Asian land temperature-related condition, this disrupts the regional condition and results in a lowered cumulative anomaly pattern correlation.

Additional ensemble sensitivity experiments were performed with the combination of warm Indian and warm Pacific acting in opposition, the warm Indian acting to increase monsoon rainfall and the warm Pacific acting to reduce monsoon rainfall. For the years this occurs in the observations (e.g., 1986, 1991, 1992, 1995, 1997), only 1992 has an opposition of sign of the single pattern correlations of significant size. However, for the model combination experiments, the regional SST forcing from the Indian Ocean dominates the Pacific, with the warm SST anomalies there producing enhanced precipitation in spite of the opposite forcing from the Pacific (not shown). This partially explains the success of the cumulative pattern correlation (Fig. 5b) and area-averaged precipitation (Fig. 5c) for 1992. The results from this experiment and the one in Fig. 12b indicate that regional forcings in this year were able to overcome opposite tendency large-scale forcings from the Pacific.

5. Case studies from observations

Another way to analyze TBO mechanisms is to choose TBO years in sequence to try and identify important processes (e.g., for the TBO sequence of years 1987–88–89 in Meehl 1997). Another is to composite TBO year sequences to look for dominant patterns related to transition mechanisms (e.g., MAL). A third is to pick representative single years to illustrate how individual transition conditions can affect monsoon precipitation, and these results are presented here. All of these types of analyses can lend physical credence to the SVD analyses, and provide insight into how the transition conditions work. In the case studies here, we will examine single years to see if effects of the transition conditions can be seen in the raw data.

Though the model experiments in this paper demonstrate how the single transition conditions can affect certain outcomes of monsoon precipitation, it therefore may be possible to see some of those features from the single conditions in the observations during years when one of them is dominant in Fig. 5a. As indicated above, this would provide another check regarding the physical plausibility of the SVD analyses in Figs. 2–4. Therefore, we choose years in Fig. 5a where one or two transition conditions were particularly strong to try and identify features in common with the SVD patterns and the model sensitivity experiments.

In Fig. 5a the year 1980 was seen to have a large contribution (+0.45) from the 500-hPa/enhanced meridional temperature gradient condition and thus should compare favorably with the SVD pattern in Fig. 2c and the model experiment in Fig. 8a. The surface vector wind anomalies and precipitation anomalies for JJAS 1980 (Fig. 13c) show positive rainfall anomalies over much of India, Bangladesh, Burma, and Southeast Asia, and southerly and southwesterly wind anomalies over the Arabian Sea. These are comparable to features in Fig. 3c for observed SVD results and the model experiment in Fig. 8a associated with the enhanced Asian meridional temperature gradient condition. There are also areas of decreased precipitation over the tropical Indian Ocean and positive precipitation anomalies in the southeast Indian Ocean in 1980 (Fig. 13c), the observed SVD (Fig. 2c), and the model experiment (Fig. 8a).

Surface temperature anomalies over south Asia in MAM 1980 reach up to +2.0°C in Fig. 13b indicative of the increased meridional temperature gradient and anomalous 500-hPa ridge over Asia (not shown). For

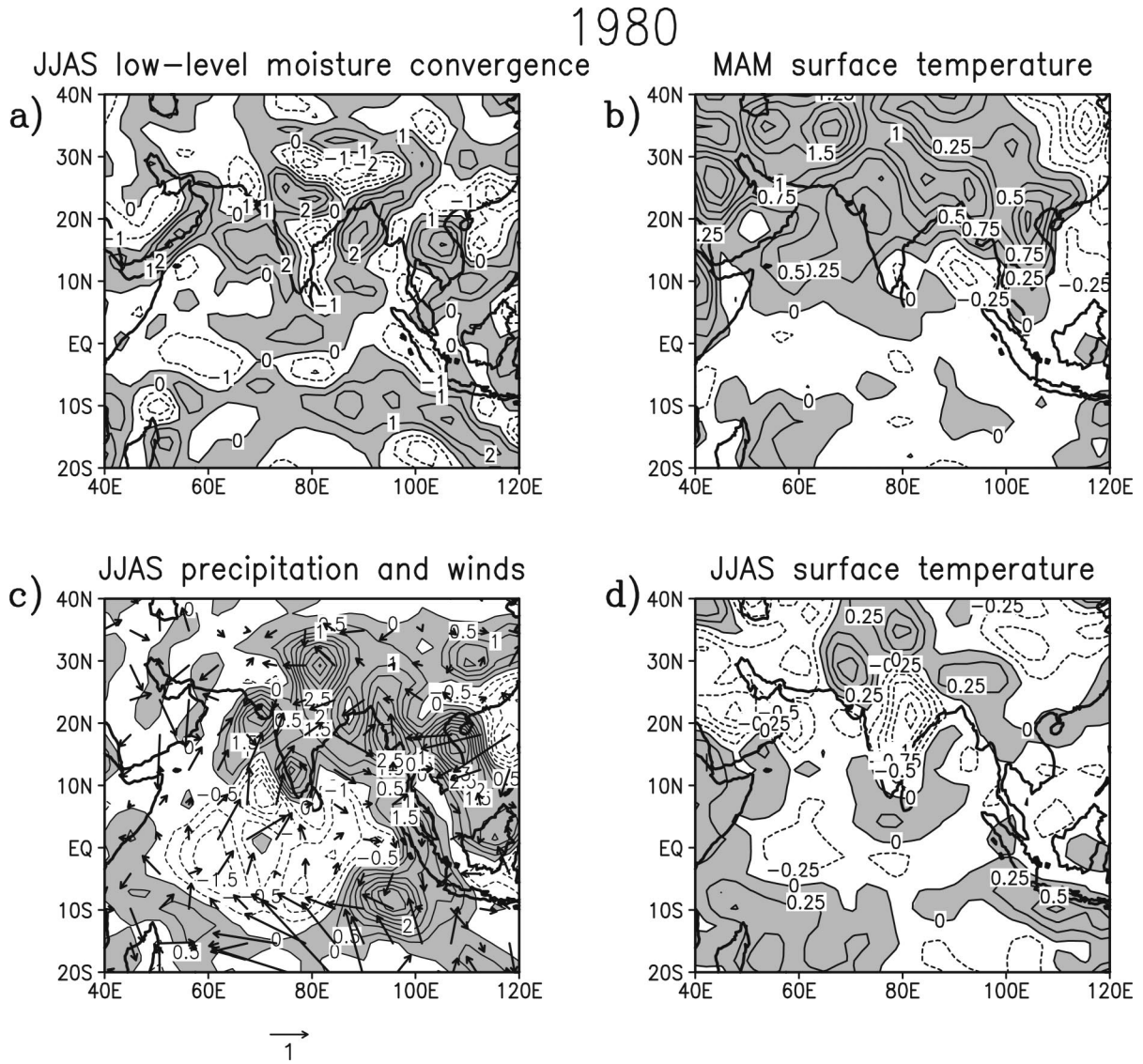

FIG. 13. Observations for 1980, (a) JJAS low-level moisture convergence anomalies (g kg^{-1} s^{-1}), (b) MAM surface temperature anomalies (°C), (c) JJAS precipitation (mm day^{-1}) and surface vector wind (scaling vector in m s^{-1}) anomalies, and (d) JJAS surface temperature anomalies (°C). Shaded areas indicate positive anomalies.

the monsoon season, the all-India rainfall index (Parthasarathy et al. 1991) for 1980 is +3% indicating slightly above-normal rainfall over India itself as part of the larger-scale enhancement over south Asian land areas, the Arabian Sea, and the Bay of Bengal in Fig. 13c. This is comparable to the corresponding GCM sensitivity experiment in Fig. 8a and the slight enhancement of area-averaged monsoon precipitation of +0.78 standard deviations. SST anomalies in the tropical Indian (Figs. 13b,d) and Pacific Oceans (not shown) are mostly less than ±0.5°C and remain that way into September–October–November (SON; not shown). Therefore, there is little contribution from anomalous SST forcing from the tropical Pacific or Indian Oceans. The precipitation anomalies are almost entirely associated with the anomalous enhanced meridional temperature gradient in MAM that produces greater low-level moisture convergence over south Asia in JJAS of 1980 (Fig. 13a).

In 1983 both the Indian SST and 500-hPa condition have high values of above +0.4 in Fig. 5a. Thus these conditions should combine to produce a cumulative pattern as was discussed in Fig. 12. Most of the Indian Ocean was anomalously warm in 1983, with positive SST anomalies nearly +0.75°C in the eastern Indian Ocean in MAM and in the western Indian Ocean in JJAS (Figs. 14b,d). Though there is a high pattern correlation value for the 500-hPa/meridional temperature gradient condition in Fig. 5a (+0.45), this is because the expansion coefficient for that condition in 1983 is negative (not shown). Therefore, there are negative sur-

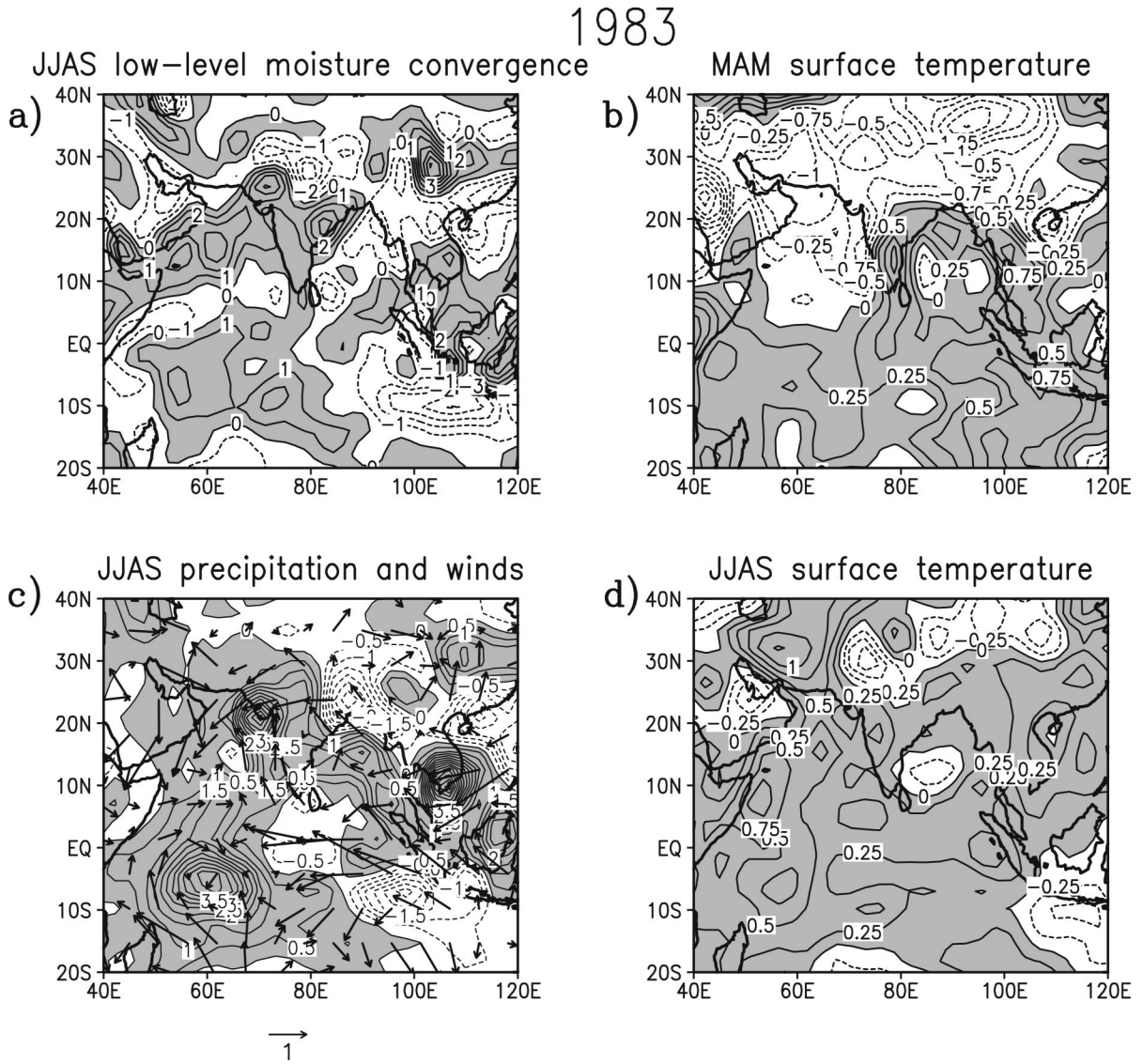

FIG. 14. Observations for 1983, (a) JJAS low-level moisture convergence anomalies (g kg^{-1} s^{-1}), (b) MAM surface temperature anomalies (°C), (c) JJAS precipitation (mm day^{-1}) and surface vector wind (scaling vector in m s^{-1}) anomalies, and (d) JJAS surface temperature anomalies (°C). Shaded values indicate positive anomalies.

face temperatures over most of south Asia in MAM (Fig. 14b). As noted above, two forcings can combine to produce the total pattern of precipitation even if one is working to weaken part of the pattern. Though SSTs are positive in the equatorial Pacific in MAM, there are a mixture of positive and negative SST anomalies in the tropical Pacific during JJAS (not shown) indicating there is little simultaneous forcing from that source (consistent with the single SVD pattern correlation value for Pacific SST in Fig. 5a of only about +0.2).

The precipitation and surface wind anomalies for JJAS 1983 are shown in Fig. 14c. Enhanced precipitation occurs over much of the tropical Indian Ocean and Indian land areas (all-India rainfall index value of +12%). This is comparable to the positive precipitation anomalies over most of these areas in the model experiment with warm Indian Ocean SSTs in Fig. 8b. Since Asian land temperatures are negative in MAM (Fig. 14b), the contribution to decreased precipitation over northeast India, Bangladesh, and Burma is likely related to this forcing. If the warm Indian Ocean SSTs were the only forcing, Fig. 8b indicates there should be enhanced rainfall in those areas. In association with the positive precipitation anomalies over most of the Indian Ocean in Fig. 14c in 1983, there are also westerly anomaly surface winds in the equatorial western Indian Ocean. Additionally, there are anomalous easterlies in the east for 1983 in Fig. 14c similar to the model simulation in Fig. 8b. These conditions in JJAS during the monsoon were set up the previous season. Low-level

moisture convergence (Fig. 14a) for JJAS 1983 shows positive values in many regions of the Indian Ocean and southern Asia in association with the anomalously warm SSTs over parts of the Indian Ocean in MAM (Fig. 14b). Thus, as in the model experiment in Fig. 8b. warm Indian Ocean SSTs result in enhanced evaporation and low-level moisture convergence, which is a moisture source for the strong monsoon. It was also noted in the SVD analysis in Fig. 3c and the model experiment in Fig. 8b that greater precipitation over much of India was associated with easterly anomaly surface winds over the Arabian Sea. This seemed to be counterintuitive for what one usually associates with greater monsoon precipitation with stronger southwesterly inflow into India over the Arabian Sea. However, in Fig. 14c there are anomalous easterly and northeasterly winds over the Arabian Sea even though there is an all-India rainfall index value of +12%. This is due to the large increases of rainfall over the tropical Indian Ocean areas in addition to greater rainfall over land and associated dynamical effects as discussed in relation to Fig. 8b.

The year 1992 has a relatively large contribution from Indian Ocean SSTs in Fig. 5a (pattern correlation value of about +0.5), and is thus chosen to illustrate conditions characterized by warm Indian Ocean SSTs south of India. This year is comparable to the model experiment in Fig. 8c. Positive SST anomalies occur in the southeastern tropical Indian Ocean in MAM (Fig. 15b) and JJAS (Fig. 15d) with values reaching +0.5°C. As noted above, this type of Indian Ocean SST pattern is more typical of a year without an ENSO onset such as 1992 (Meehl and Arblaster 2002). In 1992 SST anomalies in the equatorial Pacific are positive in MAM but are mixed in that region in JJAS (not shown). Thus it is quite comparable to the model experiment in Fig. 8c.

The observed precipitation anomalies in Fig. 15c show positive precipitation anomalies over most of the equatorial Indian Ocean. However, there are mostly negative anomalies over India and south Asia (the all-India precipitation index anomaly for 1992 was about −10% indicating weak monsoon precipitation over India itself). There are easterly and northeasterly anomaly surface winds in JJAS crossing southern India and extending into the Arabian Sea (Fig. 15c). These surface wind anomalies are indicative of the influence of the warm tropical Indian Ocean SSTs as shown by the model experiment in Fig. 8c. The model shows easterly anomaly winds over India and the Arabian Sea are the result of the warm SSTs to the south as the low-level flow converges into the region with warm SSTs and positive precipitation anomalies. Similarly, there are anomalous westerlies during JJAS in the equatorial eastern Indian Ocean in both 1992 (Fig. 15c) and in the model simulation (Fig. 8c). This is related to enhanced low-level moisture convergence over the Indian Ocean between the equator and 10°S, and near 10°N in the model (Fig. 9c) and in the observations (Fig. 15a).

The year 1988 is chosen to be representative of the cold tropical Pacific SST condition, with a large value for the Pacific SST SVD single pattern correlation coefficient in Fig. 5a of +0.65. JJAS SST anomalies in the tropical eastern Pacific are greater than −2°C in Fig. 16b, with near-zero SST anomalies in the tropical Indian Ocean. The observed 1988 precipitation (Fig. 16a) and surface wind anomalies (Fig. 16b) are similar in many respects to the model simulation in Fig. 8d, with enhanced precipitation over much of the tropical Indian Ocean and parts of India, and westerly surface wind anomalies in the western equatorial Indian Ocean. The all-India monsoon rainfall index for 1988 was +12% indicating enhanced rainfall over India itself. Figure 16a indicates that the enhanced rainfall extended over a much larger region and also included most of the tropical Indian Ocean. This is consistent with the large-scale forcing from tropical Pacific SSTs in the model experiment in Fig. 8d. As in the model experiment, the mechanism for the monsoon enhancement is large-scale east–west circulation anomalies in the atmosphere. Figure 16c shows vertical velocity (omega) anomalies for JJAS 1988 averaged from 10°S to 25°N. The positive values (anomalous downward motion) over the cold SST anomalies in the eastern Pacific occur in association with the negative values (anomalous upward motion) in the Indian monsoon region in a similar fashion to the model experiment in Fig. 11. Values greater than -1.5 g kg^{-1} s^{-1} in the midtroposphere in the monsoon longitudes of around 70°E in JJAS 1988 in Fig. 16c are comparable to values in the model simulation in Fig. 11.

The earlier results from the model experiments show that the various conditions examined earlier for the observations can, by themselves, cause a monsoon transition. They even can be seen to work in some individual years in the observations. They are not independent as noted by Meehl and Arblaster (2001, 2002) from the SVD analyses and shown earlier in Figs. 2, 3, 4, and 5. However, in any given year they can act singly or in combination to produce the actual pattern of monsoon precipitation, thus pointing to the utility of the single pattern correlation calculations in Fig. 5a to quantify the relative contributions of each condition year by year in the observations.

6. Conclusions

Earlier SVD analyses of observations by Meehl and Arblaster (2001, 2002) identified three conditions in MAM that contributed to subsequent Indian monsoon strength. These were proposed to be associated with a ''transition'' in the TBO, that is, a change in the sense of the monsoon strength from relatively weak the year before to relatively strong, or vice versa. Though it is possible to statistically quantify the relative contributions of these conditions each year, they were shown to be interrelated. Therefore, individual and cumulative SVD-related pattern correlations were used to show they could either act in unison or independently, depending

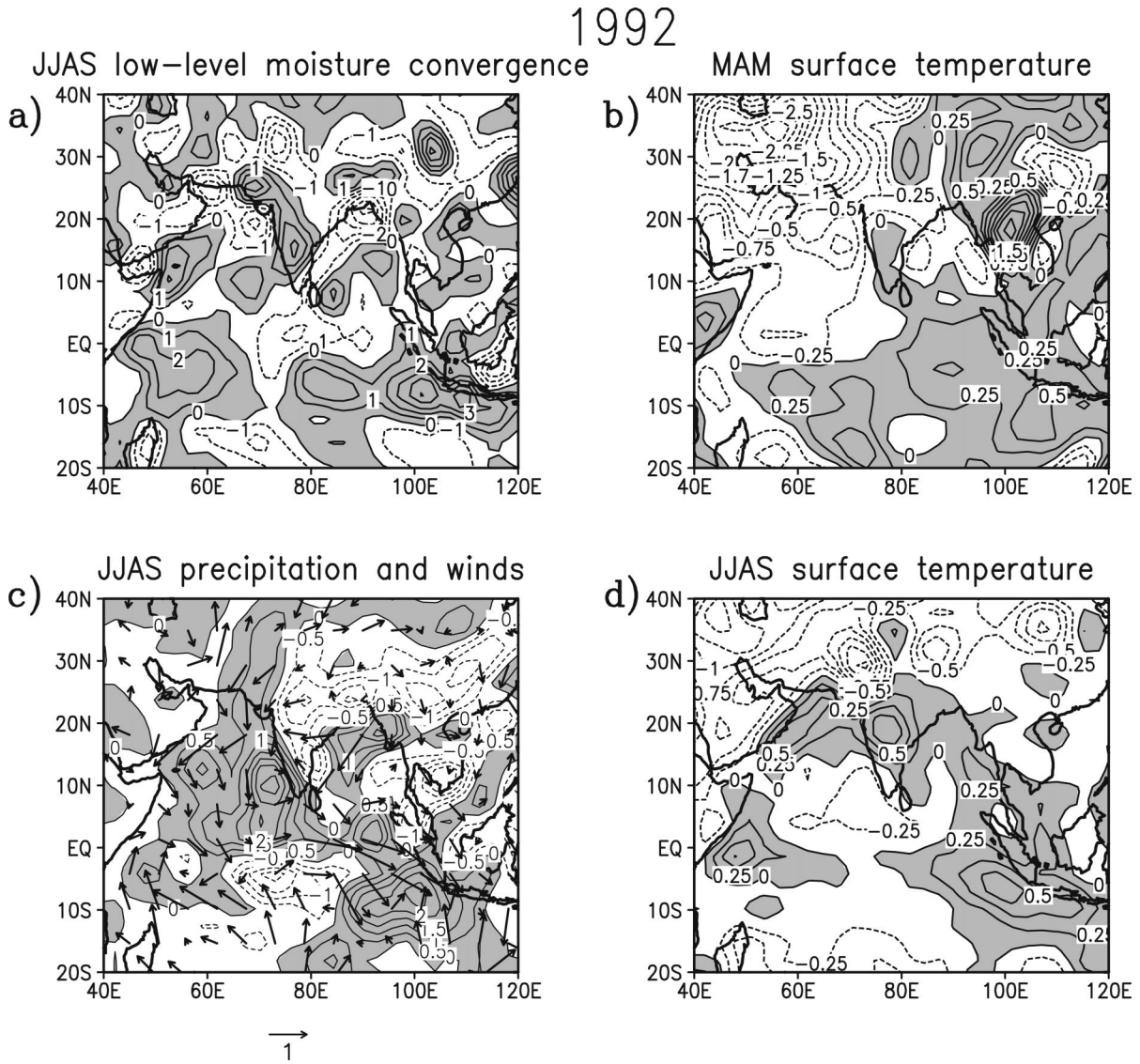

FIG. 15. Observations for 1992, (a) JJAS low-level moisture convergence anomalies (g kg^{-1} s^{-1}), (b) MAM surface temperature anomalies (°C), (c) JJAS precipitation (mm day^{-1}) and surface vector wind (scaling vector in m s^{-1}) anomalies, and (d) JJAS surface temperature anomalies (°C). Shaded areas indicate positive values.

on the year. Yet the question remained regarding whether each condition, by itself, was physically distinct and could cause a monsoon transition.

To more definitively isolate the effect on the Indian monsoon of the individual transition conditions, we perform GCM ensemble sensitivity experiments with the NCAR CCM3. The sensitivity experiments are designed to focus on each of the conditions and their contributions to Indian monsoon rainfall in JJAS. The model results are compared to the earlier SVD results from observations as well as to case studies from individual years in the observations to illustrate the following results.

1) Positive Asian land surface temperature anomalies and associated enhanced tropospheric meridional temperature gradients produce enhanced monsoon precipitation over parts of south Asia extending to the east as part of an enhanced northern summer ITCZ.
2) Positive Indian Ocean SST anomalies north of 10°S in MAM and JJAS produce a low-level moisture source with increased latent heat flux and significantly increased monsoon rainfall over a large area of the tropical Indian Ocean and south Asian land areas.
3) The location of Indian Ocean SST anomalies is important for the pattern of monsoon rainfall. If the SST anomalies are centered more near the equatorial Indian Ocean south of India, monsoon precipitation

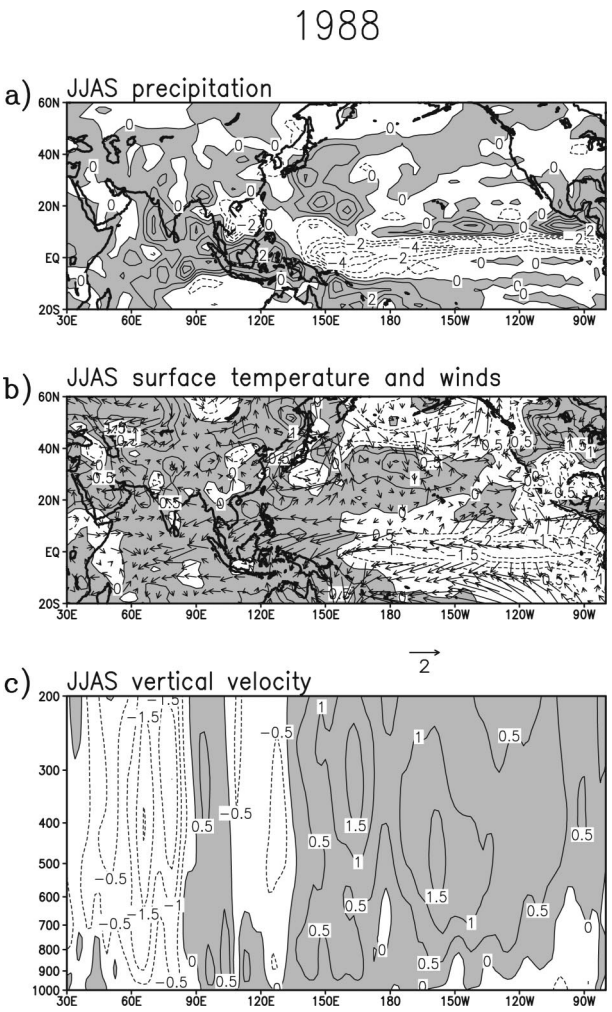

FIG. 16. Observations for 1988, (a) JJAS precipitation (mm day^{-1}) anomalies, (b) JJAS surface temperature (°C) and surface vector wind (scaling vector is 2 m s^{-1}) anomalies, and (c) JJAS vertical velocity (omega) anomalies, 15°S–25°N (hPa s^{-1}). Shaded areas indicate positive values.

will be increased over ocean areas south of India with suppressed precipitation over India itself.

4) Negative eastern equatorial Pacific SST anomalies produce enhanced Indian monsoon rainfall through the anomalous large-scale east–west atmospheric circulation, with anomalous sinking over the cold SSTs and rising motion and associated increased rainfall to the west extending over the Indian sector.
5) Additional experiments combining some of the conditions show that their effects are, to a first order, cumulative, and the influences of each can be identified in these combined experiments with the model and in case studies from observations. However, the strongest forcings over the largest areas of south Asian land and Indian Ocean involve anomalous SSTs in the Indian or Pacific Oceans.

Therefore, the transition conditions can, by themselves, affect Indian monsoon rainfall due to distinct physical processes associated with each as elucidated in the GCM experiments. They also can have varying contributions to the patterns of rainfall in any given monsoon season, thus necessitating accounting for all of them in monsoon analyses or model simulations.

Acknowledgments. A portion of this study was supported by the Office of Biological and Environmental Research, U.S. Department of Energy, as part of its Climate Change Prediction Program.

REFERENCES

Allan, R. J., and R. D. D'Arrigo, 1999: 'Persistent' ENSO sequences: How unusual was the 1990–95 El Nino? *Holocene,* **9,** 101–118.

Bonan, G. B., 1998: The land surface climatology of the NCAR Land Surface Model coupled to the NCAR Community Climate Model (CCM3). *J. Climate,* **11,** 1307–1326.

Chandrasekar, A., and A. Kitoh, 1998: Impact of localized sea surface temperature anomalies over the equatorial Indian Ocean on the Indian summer monsoon. *J. Meteor. Soc. Japan,* **76,** 841–853.

Chang, C. P., and T. Li, 2000: A theory for the tropical tropospheric biennial oscillation. *J. Atmos. Sci.,* **57,** 2209–2224.

Clark, C. O., J. E. Cole, and P. J. Webster, 2000: Indian Ocean SST and Indian summer rainfall: Predictive relationships and their decadal variability. *J. Climate,* **13,** 2503–2519.

Clarke, A. J., and L. Shu, 2000: Quasi-biennial winds in the far western equatorial Pacific phase-locking El Niño to the seasonal cycle. *Geophys. Res. Lett.,* **27,** 771–774.

——, X. Liu, and S. van Gorder, 1998: Dynamics of the biennial oscillation in the equatorial Indian and far western Pacific Oceans. *J. Climate,* **11,** 987–1001.

Gadgil, S., S. Sajani, and participating AMIP modelling groups,1998: Monsoon precipitation in AMIP runs: Results from an AMIP diagnostic subproject. World Climate Research Programme, WCRP-100, WMO/TD-837, 28 pp. and 17 figures. [Available from WCRP, c/o World Meteorological Organization, Case Postale No. 2300, CH-1211 Geneva 2, Switzerland.]

Ju, J., and J. Slingo, 1995: The Asian summer monsoon and ENSO. *Quart. J. Roy. Meteor. Soc.,* **121,** 1133–1168.

Kalnay, E., and Coauthors, 1996: The NCEP/NCAR 40-Year Reanalysis Project. *Bull. Amer. Meteor. Soc.,* **77,** 437–471.

Kang, I.-S., and Coauthors, 2001: Intercomparison of GCM simulated anomalies associated with the 1997–98 El Niño event. *J. Climate,* submitted.

Kiehl, J. T., J. J. Hack, G. Bonan, B. Boville, D. Williamson, and P. Rasch, 1998: The National Center for Atmospheric Research Community Climate Model (CCM3). *J. Climate,* **11,** 1131–1149.

Kim, K.-M., and K.-M. Lau, 2001: Dynamics of monsoon-induced biennial variability in ENSO. *Geophys. Res. Lett.,* **28,** 315–318.

Lal, M., G. A. Meehl, and J. M. Arblaster, 2000: Simulation of Indian summer monsoon rainfall and its intraseasonal variability. *Reg. Environ. Change,* **1,** 163–179.

Lau, K.-M., and W. Bua, 1998: Mechanisms of monsoon–Southern Oscillation coupling: Insights from GCM experiments. *Climate Dyn.,* **14,** 759–779.

——, and H.-T. Wu, 1999: Assessment of the impacts of the 1997–98 El Niño on the Asian–Australia monsoon. *Geophys. Res. Lett.,* **26,** 1747–1750.

Li, C., and M. Yanai, 1996: The onset and interannual variability of the Asian summer monsoon in relation to land–sea thermal contrast. *J. Climate,* **9,** 358–375.

Meehl, G. A., 1987: The annual cycle and interannual variability in the tropical Indian and Pacific Ocean regions. *Mon. Wea. Rev.,* **115,** 27–50.

——, 1993: A coupled air–sea biennial mechanism in the tropical

Indian and Pacific regions: Role of the ocean. *J. Climate,* **6,** 31–41.
——, 1994: Coupled land–ocean–atmosphere processes and south Asian monsoon variability. *Science,* **266,** 263–267.
——, 1997: The south Asian monsoon and the tropospheric biennial oscillation. *J. Climate,* **10,** 1921–1943.
——, and J. Arblaster, 1998: The Asian–Australian monsoon and El Niño–Southern Oscillation in the NCAR climate system model. *J. Climate,* **11,** 1357–1387.
——, and ——, 2001: The tropospheric biennial oscillation and Indian monsoon rainfall. *Geophys. Res. Lett.,* **28,** 1731–1734.
——, and ——, 2002: The tropospheric biennial oscillation and Asian–Australian monsoon rainfall. *J. Climate,* **15,** 722–744.
——, ——, and J. Loschnigg, 2002: Coupled ocean–atmosphere processes in the tropical Indian and Pacific Ocean regions and the TBO. *J. Climate,* submitted.
Palmer, T. N., C. Brankovic, P. Viterbo, and M. J. Miller, 1992: Modeling interannual variations of summer monsoons. *J. Climate,* **5,** 399–417.
Parthasarathy, B., K. Rupa Kumar, and A. A. Munot, 1991: Evidence of secular variations in Indian monsoon rainfall–circulation relationships. *J. Climate,* **4,** 927–938.
Rao, K. G., and B. N. Goswami, 1988: Interannual variations of the sea-surface temperature over the Arabian Sea and the Indian monsoon: A new perspective. *Mon. Wea. Rev.,* **116,** 558–568.
Rasmusson, E. M., and T. H. Carpenter, 1983: The relationship between eastern equatorial Pacific sea surface temperatures and rainfall over India and Sri Lanka. *Mon. Wea. Rev.,* **111,** 517–528.
Shukla, J., 1975: Effect of Arabian sea-surface temperature anomaly on Indian summer monsoon: A numerical experiment with the GFDL model. *J. Atmos. Sci.,* **32,** 503–511.
——, and D. A. Paolino, 1983: The Southern Oscillation and long-range forecasting of the summer monsoon rainfall over India. *Mon. Wea. Rev.,* **111,** 1830–1837.
Soman, M. K., and J. Slingo, 1997: Sensitivity of Asian summer monsoon to aspects of sea surface temperature anomalies in the tropical Pacific Ocean. *Quart. J. Roy. Meteor. Soc.,* **123,** 309–336.
Tomita, T., and T. Yasunari, 1996: Role of the northeast winter monsoon on the biennial oscillation of the ENSO/monsoon system. *J. Meteor. Soc. Japan,* **74,** 399–413.
Trenberth, K. E., D. P. Stepaniak, and J. W. Hurrell, 2001: Quality of reanalyses in the Tropics. *J. Climate,* **14,** 1499–1510.
Washington, W. M., R. M. Chervin, and G. V. Rao, 1977: Effects of a variety of Indian Ocean surface temperature anomaly patterns on the summer monsoon circulation: Experiments with the NCAR general circulation model. *Pure Appl. Geophys.,* **115,** 1335–1356.
Webster, P. J., V. O. Magana, T. N. Palmer, J. Shukla, R. A. Tomas, M. Yanai, and T. Yasunari, 1998: Monsoons: Processes, predictability, and the prospects for prediction. *J. Geophys. Res.,* **103,** 14 451–14 510.
——, A. M. Moore, J. P. Loschnigg, and R. R. Leben, 1999: Coupled ocean–atmosphere dynamics in the Indian Ocean during 1997–98. *Nature,* **401,** 356–360.
Xie, P., and P. A. Arkin, 1996: Analyses of global monthly precipitation using gauge observations, satellite estimates, and numerical model predictions. *J. Climate,* **9,** 840–858.
Yamazaki, K., 1988: Influence of sea surface temperature anomalies over the Indian Ocean and Pacific Ocean on the tropical atmospheric circulation: A numerical experiment. *J. Meteor. Soc. Japan,* **66,** 797–806.
Yang, S., and K.-M. Lau, 1998: Influences of sea surface temperature and ground wetness on Asian summer monsoon. *J. Climate,* **11,** 3230–3246.
——, ——, and M. Sankar-Rao, 1996: Precursory signals associated with the interannual variability of the Asian summer monsoon. *J. Climate,* **9,** 949–964.
Yasunari, T., and Y. Seki, 1992: Role of the Asian monsoon on the interannual variability of the global climate system. *J. Meteor. Soc. Japan,* **70,** 177–189.